

Article

Involvement of Differentially Expressed microRNAs in the PEGylated Liposome Encapsulated ¹⁸⁸Rhenium-Mediated Suppression of Orthotopic Hypopharyngeal Tumor

Bing-Ze Lin ^{1,†}, Shen-Ying Wan ^{1,2,†}, Min-Ying Lin ¹, Chih-Hsien Chang ^{1,3},
Ting-Wen Chen ^{4,5,6} , Muh-Hwa Yang ^{7,8,9} and Yi-Jang Lee ^{1,7,*} 

¹ Department of Biomedical Imaging and Radiological Sciences, National Yang-Ming University, No. 155, Sec. 2, Linong St. Beitou District, Taipei 11221, Taiwan; innovationmark1012@gmail.com (B.-Z.L.); sywang@mail.femh.org.tw (S.-Y.W.); milo841120@gmail.com (M.-Y.L.); chchang@iner.gov.tw (C.-H.C.)

² Department of Nuclear Medicine, Far Eastern Memorial Hospital, New Taipei City 22000, Taiwan

³ Isotope Application Division, Institute of Nuclear Energy Research, Taoyuan 32546, Taiwan

⁴ Institute of Bioinformatics and Systems Biology, National Chiao Tung University, Hsinchu 30068, Taiwan; dodochen@nctu.edu.tw

⁵ Department of Biological Science and Technology, National Chiao Tung University, Hsinchu 30068, Taiwan

⁶ Center For Intelligent Drug Systems and Smart Bio-devices (IDS2B), National Chiao Tung University, Hsinchu 30068, Taiwan

⁷ Cancer Progression Research Center, National Yang-Ming University, Taipei 11221, Taiwan; mhyangymu@gmail.com

⁸ Institute of Clinical Medicine, National Yang-Ming University, Taipei 11221, Taiwan

⁹ Division of Medical Oncology, Department of Oncology, Taipei Veteran General Hospital, Taipei 11217, Taiwan

* Correspondence: yjlee2@ym.edu.tw

† These authors contributed equally to this work.

Academic Editor: Krishan Kumar

Received: 30 June 2020; Accepted: 6 August 2020; Published: 8 August 2020



Abstract: Hypopharyngeal cancer (HPC) accounts for the lowest survival rate among all types of head and neck cancers (HNSCC). However, the therapeutic approach for HPC still needs to be investigated. In this study, a theranostic ¹⁸⁸Re-liposome was prepared to treat orthotopic HPC tumors and analyze the deregulated microRNA expressive profiles. The therapeutic efficacy of ¹⁸⁸Re-liposome on HPC tumors was evaluated using bioluminescent imaging followed by next generation sequencing (NGS) analysis, in order to address the deregulated microRNAs and associated signaling pathways. The differentially expressed microRNAs were also confirmed using clinical HNSCC samples and clinical information from The Cancer Genome Atlas (TCGA) database. Repeated doses of ¹⁸⁸Re-liposome were administrated to tumor-bearing mice, and the tumor growth was apparently suppressed after treatment. For NGS analysis, 13 and 9 microRNAs were respectively up-regulated and down-regulated when the cutoffs of fold change were set to 5. Additionally, miR-206-3p and miR-142-5p represented the highest fold of up-regulation and down-regulation by ¹⁸⁸Re-liposome, respectively. According to Differentially Expressed MiRNAs in human Cancers (dbDEMC) analysis, most of ¹⁸⁸Re-liposome up-regulated microRNAs were categorized as tumor suppressors, while down-regulated microRNAs were oncogenic. The KEGG pathway analysis showed that cancer-related pathways and olfactory and taste transduction accounted for the top pathways affected by ¹⁸⁸Re-liposome. ¹⁸⁸Re-liposome down-regulated microRNAs, including miR-143, miR-6723, miR-944, and miR-136 were associated with lower survival rates at a high expressive level. ¹⁸⁸Re-liposome could suppress the HPC tumors in vivo, and the therapeutic efficacy was associated with the deregulation of microRNAs that could be considered as a prognostic factor.

Keywords: hypopharyngeal cancer; ^{188}Re -liposome; repeated therapy; NGS; microRNA

1. Introduction

Hypopharyngeal cancer (HPC) represents malignant growth in the hypopharynx region and accounts for about 5% of all head and neck cancers (HNSCC) [1]. As HPC is a rare cancer type with a late occurrence of symptoms and tumor spreading, it is not uncommon for it to be detected at advanced stages with a high mortality rate and poor prognosis [2]. HPC can be treated by conventional surgery, radiotherapy and chemotherapy, while radiotherapy alone is usually used at an early stage [3]. On the other hand, a combination of different therapeutic modalities can improve the five-year survival of this disease [4]. Several lines of evidence have claimed that a combination of radiotherapy and chemotherapy would provide better control of locoregional recurrence compared to surgical procedures [4,5]. A radiopharmaceutical named $^{99\text{m}}\text{Tc}$ -MIBI (methoxy-isobutyl-isonitrile) has been reported to detect HPC with up to a 95% sensitivity using single photon emission computed tomography (SPECT) [6]. However, nuclear medicine has not been reported to have assessed or monitored the efficacy of HPC therapy as mentioned above.

Radiopharmaceuticals are not only used for diagnostic purposes but also therapeutic purposes, so-called radiotheranostics [7]. Rhenium-188 (^{188}Re) belongs to this type of radionuclide as it emits 85% high-energy β -particles (2.12MeV) and 15% γ -rays (155keV) [8]. The average soft tissue penetration distance of β -particles is only around 3.8mm, suggesting that ^{188}Re is suitable for tumor ablation and will not have significant side effects on distant normal tissues [9,10]. ^{188}Re has been conjugated to hydroxyethylidene diphosphonate (HEDP) for bone pain palliation [11,12]. The antibody conjugated ^{188}Re has also been reported to treat different cancers [13]. Additionally, low immunogenic peptides such as somatostatin derivative conjugated ^{188}Re , have been investigated in clinics for patients with advanced pulmonary cancer [14]. ^{188}Re -labeled lipiodol and microspheres were used for the treatment of hepatocellular carcinoma [15–17]. ^{188}Re -labelled radiocolloids have also been developed to treat skin cancers within a brachytherapy device [18]. ^{188}Re -loaded lipid nanocapsules, also called ^{188}Re -liposome, have been demonstrated to be biocompatible and subjected to a phase 0 clinical study for patients with metastatic tumors [19]. ^{188}Re -liposome has shown a theranostic efficacy in various human cancers, including colorectal cancer, glioblastomas, lung cancer, ovarian cancer, esophageal cancer and head and neck cancer using xenograft tumor models [20–26]. The molecular mechanisms of rhenium-188 labelled radiopharmaceuticals are of interest for investigation aimed at interpreting the potent therapeutic efficacy.

Radiogenomics is defined as connecting radiomics and genetic profiles to apply the feature of medical imaging in radiation-mediated molecular responses [27]. The purpose of this discipline is to predict the association between gene expression and the radiotherapy-induced toxic effects of tumors [28]. Next-generation sequencing (NGS) analysis is the most cutting-edge technology that can decipher dramatic amounts of gene expressive alterations in tumors, with or without therapies [29,30]. NGS applications include RNA sequencing (RNA-Seq) that can analyze the expression of various RNA populations (mRNA, microRNA, long non-coding RNA, etc.) and their modification forms generated from alternative splicing, mutations or gene fusion [31]. Compared to the conventional cDNA expression microarray, RNA-Seq has a broader spectrum for finding novel and unidentified transcripts [32]. This method is important for providing more detailed and quantitative data for bioinformatics analysis of genetic profiling in novel drug development and predicting the signaling pathways of toxicity and therapeutic effects [33]. As a radioactive compound, ^{188}Re -liposome is believed to influence the genetic profile of tumors. However, related studies have rarely been reported.

In this study, we investigated the effects of ^{188}Re -liposome on the miRNA expressive profiles of HPC derived xenograft tumors using RNA-Seq technology. The changed miRNA profiles were analyzed using the Kyoto Encyclopedia of Genes and Genomes (KEGG) pathway database and Ingenuity Pathway

Analysis (IPA). The total expressive amount of miRNA from ^{188}Re -liposome-treated tumors was about 10% lower than that of untreated tumor. The changed miRNA profile led to 4498 differentially expressed genes (DEGs) that influenced 30 molecular pathways, including olfactory transduction, the cancer pathway, and taste transduction, which accounted for the top three pathways. We also found that ^{188}Re -liposome up-regulated several tumor suppressor microRNAs, such as miR-34-5p, miR-193a-5p, miR-125b-5p, miR-133a-5p, and miR-133b-5p. Concomitantly, several oncomirs, including miR-21-5p, miR-32-5p and miR-205-5p were down-regulated by ^{188}Re -liposome. An online Kaplan-Meier (K-M) plotter with The Cancer Genome Atlas (TCGA) database was also used to compare the expression of these miRNA and the survival of head and neck cancer patients. The results of ^{188}Re -liposome-induced miRNA dysregulation detected by RNA-Seq were discussed.

2. Results

2.1. Effects of ^{188}Re -Liposome on HPC Derived Orthotopic Tumors Using the Repeated Dose Regime

A flowchart of ^{188}Re -liposomal manufacturing and the chemical structures of the ^{188}Re -perrhenate precursor and BMEDA chelator are illustrated in Figure 1. The timeline was schemed for the establishment of HPC tumor-bearing mice using FaDu-3R cells (Supplementary Figure S2), the administration of ^{188}Re -liposome, the optical imaging of tumor responses, tumor resection for RNA extraction, and NGS analysis (Figure 2A). The growth of orthotopic tumors was significantly suppressed by ^{188}Re -liposome but not saline as detected using bioluminescent imaging (Figure 2B,C). The size of resected tumors also exhibited obvious differences between the saline control and ^{188}Re -liposome-treated mice after 30 days of initial implantation (Figure 2D). The body weights of tumor-bearing mice were not significantly affected by ^{188}Re -liposome (Figure 2E). Furthermore, we showed that DNA damage marker γ -H2AX was significantly up-regulated by ^{188}Re -liposome treatment (Figure 2F,G). These data suggest that the regime of ^{188}Re -liposome treatment with repeated doses exhibited therapeutic efficacy, with little systemic toxicity.

2.2. Use of NGS Analysis to Investigate the microRNA Expressive Profile of HPC Tumor Treated with ^{188}Re -Liposome

The resected FaDu HPC tumors treated with saline or repeated doses of ^{188}Re -liposome were subjected to RNA extraction to obtain a high quality of total RNA for RNA-seq analysis (Supplementary Figure S3). The quality of raw data obtained by this analysis was determined by the GC content, by which the raw data quality of the saline control and ^{188}Re -liposome-treated tumor was shown to be similar (Supplementary Figure S4). To confirm the expressive change in microRNA in tumors treated with or without ^{188}Re -liposome, the reads number of small RNA (15–55 mers) was extracted and counted using a Small RNA Analysis tool (see Materials and Methods). The average lengths of small RNA after extraction were 32.9 and 32 mers for the control and ^{188}Re -liposome treated tumor, respectively. Under this condition, the total reads number of the control and ^{188}Re -liposome treated tumor was 10,612,998 and 9,844,775, respectively. The reads were then subjected to the miRBase database (release 21) for the annotation of small RNA using the Annotate and Merge Count of Small RNA Analysis software. The annotated small RNAs of saline-treated tumors and ^{188}Re -liposome treated tumors were 639 and 572, respectively. The differentially expressed microRNAs were clustered in a heatmap for a comparison of saline-treated and ^{188}Re -liposome treated HPC tumor models (Supplementary Figure S5). Furthermore, we set the cutoff at five-fold change (\log_2) of microRNA and showed that 13 microRNA and 9 microRNA with mature forms were up-regulated and down-regulated by ^{188}Re -liposome normalized to the saline control, respectively (Table 1). The 13 up-regulated microRNAs ranked from highest to lowest fold change were miR-206-3p, mir668-3p, mit-485-3p, miR-382-5p, miR-1268b-5p, miR-193a-5p, miR-7-1-5p, miR-378a-5p, miR-1266-5p, miR-4510-5p, miR-370-3p, miR-34a-5p, and miR-342-5p. The nine down-regulated microRNAs ranked from highest to lowest fold change were miR-142-5p, miR-6723-5p, miR-944-3p, miR-142-3p, miR-136-3p,

miR-151b-3p, miR-194-2-5p, miR-143-5p, and miR-3960-3p. According to the online analysis of dbDEMCC, ^{188}Re -liposome-up-regulated microRNAs were mostly naturally down-regulated in HNSCC and were predicted as tumor suppressors (Table 2). MiR-193a, miR-7-1-5p and miR-342-5p were up-regulated in HNSCC, but could still be tumor suppressors in different types of cancer (see references in Table 2). For the nine ^{188}Re -liposome down-regulated microRNAs, only four of them (miR-136-3p, miR-142-3p, miR-944-3p, and miR-142-5p) were reported in the HNSCC of dbDEMCC database. Interestingly, three out of these four microRNAs were found to be up-regulated in HNSCC and predicted as oncogenes (Table 3). However, most of the ^{188}Re -liposome-down-regulated microRNAs contain oncogenic properties (see references in Table 3). These results suggested that the therapeutic efficacy of ^{188}Re -liposome was associated with the deregulation of tumor-suppressive and/or oncogenic microRNAs.

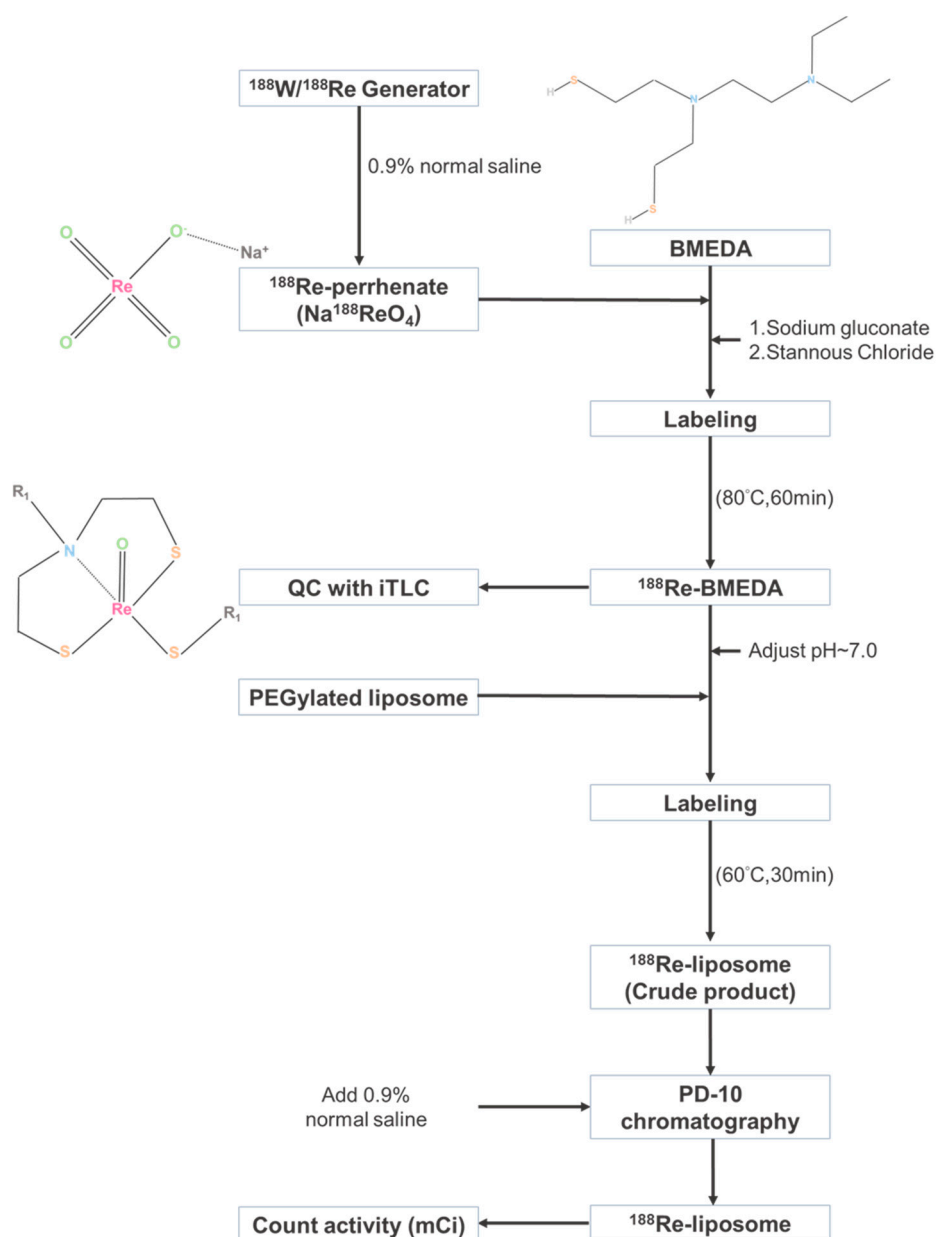


Figure 1. The flowchart of ^{188}Re -liposomal preparation. The chemical structures of $\text{Na}^{188}\text{ReO}_4$, BMEDA and formed ^{188}Re -BMEDA were also illustrated.

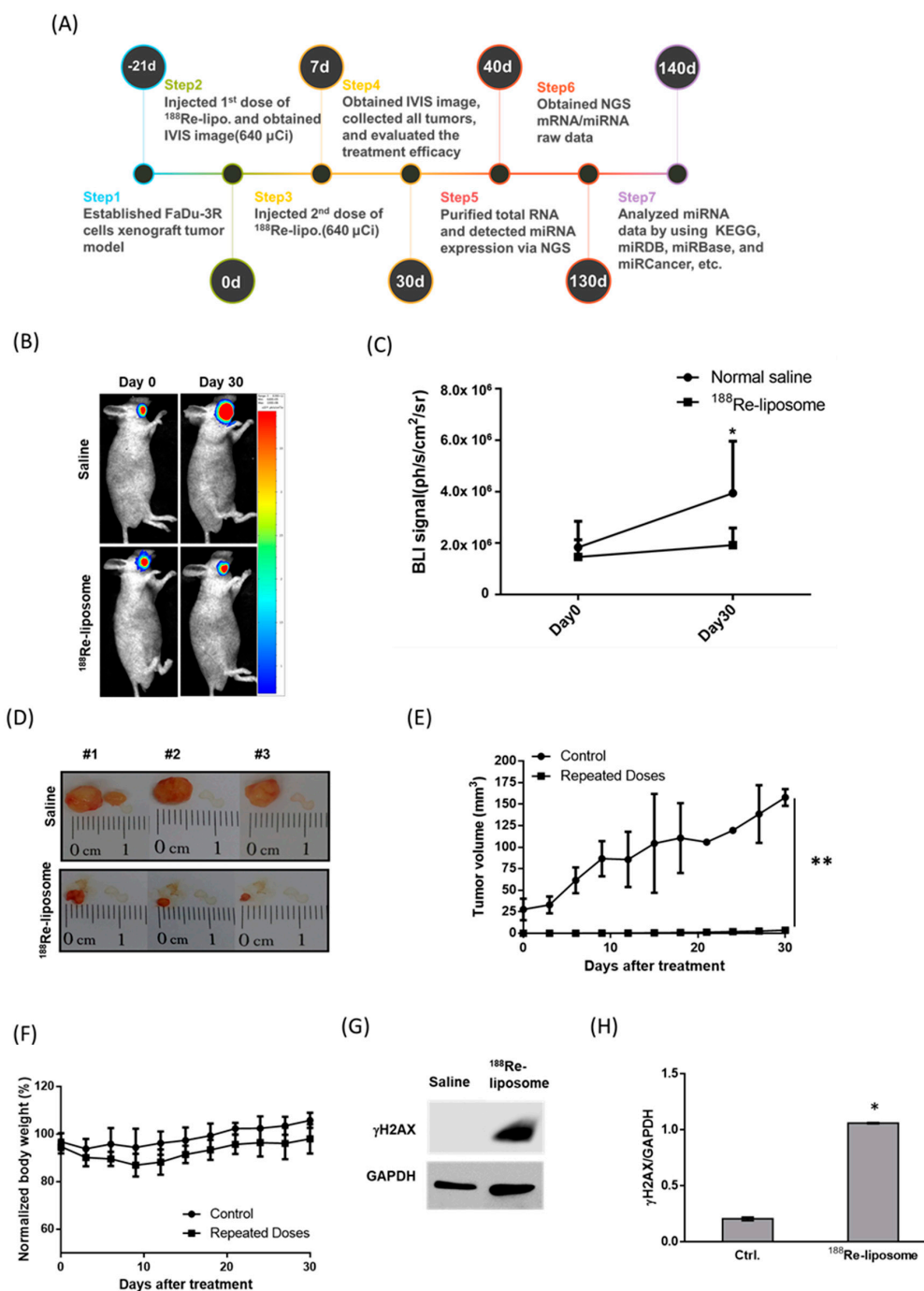


Figure 2. Comparison of PEGylated ¹⁸⁸Re-liposomal accumulation in orthotopic hypopharyngeal cancer (HPC) tumors after repeated injections. (A) The experimental scheme for ¹⁸⁸Re-liposome treatment and analysis. (B) Reporter gene imaging of tumor growth responding to repeated doses of ¹⁸⁸Re-liposome, and the saline-treated control. (C) Quantification of bioluminescent imaging (BLI) signals. *: $p < 0.05$. (D) Representative photos of excised orthotopic tumors with or without the treatment of ¹⁸⁸Re-liposomes. (E) Caliper measurement of tumor volumes. Data are represented as means \pm S.D. **: $p < 0.01$. (F) Measurement of body weights of mice. (G) Comparison of the γ -H2AX protein expression in tumors with or without the treatment of ¹⁸⁸Re-liposomes. (H) Densitometric quantification of Western blots. *: $p < 0.05$.

Table 1. Expression of microRNAs in human hypopharyngeal tumor model treated with ¹⁸⁸Re-liposome.

MicroRNA	Fold Change (¹⁸⁸ Re-lipo./Ctrl.) ^a	Ctrl. Norm. by TMM ^b	¹⁸⁸ Re-lipo. Norm. by TMM	Ctrl. RPM ^c	¹⁸⁸ Re-lipo. RPM
Hsa-miR-206-3p	40.19	76.05	3056.53	2.92	90.71
Hsa-miR-668-3p	11.16	2.45	27.38	0.09	0.81
Hsa-miR-485-3p	9.77	2.45	23.96	0.09	0.71
Hsa-miR-382-5p	9.15	22.08	201.94	0.85	5.99
Hsa-miR-1268b-5p	8.37	2.45	20.54	0.09	0.61
Hsa-miR-193a-5p	6.28	4.91	30.8	0.19	0.91
Hsa-miR-7-1-5p	6.28	9.81	61.61	0.38	1.83
Hsa-miR-378a-5p	5.78	51.52	297.78	1.98	8.84
Hsa-miR-1266-5p	5.58	2.45	13.69	0.09	0.41
Hsa-miR-4510-5p	5.58	2.45	13.69	0.09	0.41
Hsa-miR-370-3p	5.58	4.91	27.38	0.19	0.81
Hsa-miR-34a-5p	5.15	127.57	657.17	4.9	19.5
Hsa-miR-342-5p	5.12	7.36	37.65	0.28	1.12
Hsa-miR-3960-3p	-5.73	117.76	20.54	4.52	0.61
Hsa-miR-143-5p	-5.73	19.63	3.42	0.75	0.1
Hsa-miR-194-2-5p	-5.73	19.63	3.42	0.75	0.1
Hsa-miR-151b-3p	-6.45	22.08	3.42	0.85	0.1
Hsa-miR-136-3p	-7.17	24.53	3.42	0.94	0.1
Hsa-miR-142-3p	-7.88	26.99	3.42	1.04	0.1
Hsa-miR-944-3p	-9.32	31.89	3.42	1.22	0.1
Hsa-miR-6723-5p	-10.03	34.35	3.42	1.32	0.1
Hsa-miR-142-5p	-10.14	242.88	23.96	9.33	0.7

^a—Fold change in microRNA over 5 or below -5 were selected. ^b—TMM: Trimmed mean of M values. ^c—RPM: Reads of exon model per million mapped reads. (ExonMappedReads × 10⁶/TotalMapped Reads).

2.3. Validation of microRNA Identified in NGS Data Using qPCR

We next used qPCR to validate up-regulated and down-regulated microRNA in the FaDu HPC tumor model treated with ¹⁸⁸Re-liposome. We selected microRNAs that displayed over five-fold deregulation with the highest RPM, including miR-206-3p, miR-382-5p, miR-378a-5p, miR-3960-3p, and miR-142-5p to be validated. The results showed that the expressive patterns of these microRNAs obtained by qPCR were consistent with the observations of NGS analysis (Figure 3).

2.4. Investigation of Differentially Expressed microRNAs in Clinical Samples

As ¹⁸⁸Re-liposome could influence the expression of certain microRNAs that may correlate with the tumor-suppressive effect of the HPC model, we were interested in examining the status of these microRNAs in clinical HNSCC tumors. First, we obtained clinical HNSCC tissues from patients (n = 6) to investigate the differential expression of microRNAs in tumor tissues and adjacent normal tissues using qPCR analysis. We selected miR-206-3p, miR-378a-5p and miR-142-5p as they exhibited the highest differential deregulation by ¹⁸⁸Re-liposome (Figure 3). The results showed that the expression of miR-206-3p and miR-378a-5p was down-regulated (Figure 4A,B), while miR-142-5p was up-regulated in tumors compared to normal tissues (Figure 4C). Additionally, we employed the clinical information of HNSCC in the TCGA database to compare the differentially expressed microRNAs in HNSCC and normal tissues. Because the number of cases of hypopharynx cancer was too low to be analyzed, here we used clinical information on larynx cancer types instead. A heatmap was generated for the microRNAs displaying over five-fold change caused by ¹⁸⁸Re-liposome (Supplementary Figure S6). Accordingly, we found that miR-206 (equivalent to miR-206-3p) and miR-378a-5p were significantly down-regulated, while miR-143-5p, miR-142-3p, and miR-944 were significantly up-regulated in tumors (Figure 4D). MiR-142-5p also exhibited a trend of up-regulation, although the significance was marginal. This suggests that ¹⁸⁸Re-liposome can reverse the expression of the microRNAs that were originally deregulated in HNSCC.

Table 2. Functional prediction algorithm for microRNAs of human hypopharyngeal tumor model up-regulated by ¹⁸⁸Re-liposome.

MiRNAs up-Regulated in HPC	Original Change in HNSCC ^a	Role Prediction	Functional Importance	GEO ID	References ^b
Hsa-miR-206-3p	down-regulation	Tumor suppressor	Weakens cell proliferation, migration, invasion, promotes S phase cell arrest. Inhibits cell aggressiveness	TCGA_HNSC	[34,35]
Hsa-miR-668-3p	down-regulation	Tumor suppressor	Induces growth arrest and premature senescence	- ^c	[36,37]
Hsa-miR-485-3p	down-regulation	Tumor suppressor	Inhibits mitochondrial biogenesis or promotes cancer growth and migration	GSE75630	[38–40]
Hsa-miR-382-5p	down-regulation	Tumor Suppressor	Promotes lymph node metastasis and TNM stage; inhibition of proliferation and EMT in glioma cells	TCGA_HNSC	[41,42]
Hsa-miR-1268b-5p	-	Tumor suppressor	Increases chemosensitivity	-	[43]
Hsa-miR-193a-5p	up-regulation	Tumor Suppressor	Suppresses the growth and the metastasis of cancer cells	TCGA_HNSC	[44,45]
Hsa-miR-7-1-5p	up-regulation	Tumor suppressor	Inhibits proliferation, invasion and induces apoptosis in cancer cells	TCGA_HNSC	[46,47]
Hsa-miR-378a-5p	down-regulation	Tumor suppressor	Inhibits cellular proliferation and colony formation.	TCGA_HNSC	[48,49]
Hsa-miR-1266-5p	down-regulation	Tumor suppressor	Induces apoptosis and reduces proliferation	TCGA_HNSC	[50,51]
Hsa-miR-4510-5p	-	Tumor suppressor	Down-regulation in recurrent cancer and a potential cancer biomarker	-	[52,53]
Hsa-miR-370-3p	down-regulation	Tumor suppressor	Potential cancer biomarker	TCGA_HNSC	[54]
Hsa-miR-34a-5p	down-regulation	Tumor suppressor	Inhibits tumorigenesis and progression	TCGA_HNSC	[55,56]
Hsa-miR-342-5p	up-regulation	Tumor suppressor	Reduces cell cycle progression	TCGA_HNSC	[57,58]

^a—The change of microRNA was determined by the dbDEMC online databases. ^b—The selected references may be not HPC or HNSCC related. ^c—The tumor suppressive function was concluded from clinical patients.

Table 3. Target prediction algorithm for microRNAs of human hypopharyngeal tumor model down-regulated by ¹⁸⁸Re-liposome.

MiRNAs Down-Regulated in HPC	Original Change in HNSCC	Role Prediction	Functional Importance	GEO ID	Reference
Hsa-miR-3960-3p	-	-	-	-	-
Hsa-miR-143-5p	-	Both	cell viability, colony formation	-	[59,60]
Hsa-miR-194-2-5p	-	Oncogene	cell proliferation, migration and invasion	-	[61,62]
Hsa-miR-151b-3p	-	Oncogene? ^a	Biomarker of sarcoma	-	[63]
Hsa-miR-136-3p	down-regulation	Oncogene	Biomarker of bladder cancer, promote cancer growth and migration	TCGA-HNSC	[64,65]
Hsa-miR-142-3p	up-regulation	Oncogene	Over-expression in OSCC, association with cancer growth and migration	TCGA-HNSC	[66,67]
Hsa-miR-944-3p	up-regulation	Oncogene	A biomarker of poor prognosis/Regulation of chemoresistance	TCGA-HNSC	[68,69]
Hsa-miR-6723-5p	-	-	-	-	-
Hsa-miR-142-5p	up-regulation	Oncogene	Deregulation of cell proliferation; SMAD3/TGF- β	GSE31277	[70,71]

^a No direct evidence, but just an implication.

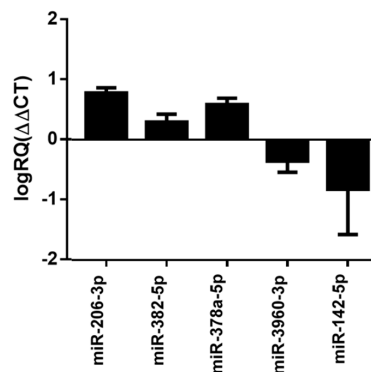


Figure 3. Validation of the next-generation sequencing (NGS) results of the HPC tumor model by qPCR analysis. The results were each microRNA of ^{188}Re -liposome-treated HPC normalized to that of untreated controls.

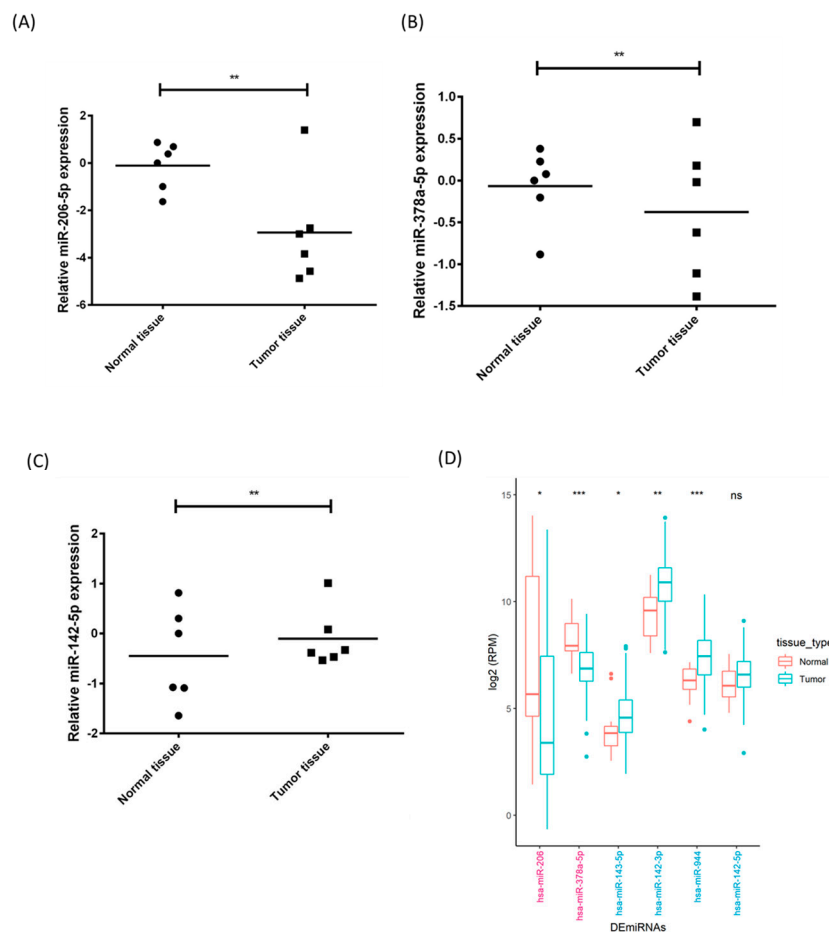


Figure 4. Comparison of the microRNA expression in clinical head and neck cancer (HNSCC) tissues and adjacent normal tissues by qPCR analysis. (A) MiR-206-3p. (B) MiR-378a-5p (C) MiR-142-5p. (D) Differentially expressed microRNA (DEmiRNA) in larynx tumor and normal tissues using the clinical information of The Cancer Genome Atlas (TCGA). *: $p < 0.05$, **: $p < 0.01$. ***: $p < 0.001$.

2.5. Prediction of Genes Targeted by ^{188}Re -Liposome-Deregulated microRNAs

We next examined the potent target genes that might be affected by ^{188}Re -liposome deregulated microRNAs. The miRDB online database was employed to rank the numbers of predicted genes targeted by microRNAs that were deregulated by ^{188}Re -liposome (see Materials and Methods). The ranking

of target numbers affected by ^{188}Re -liposome up-regulated and down-regulated microRNAs was obtained, respectively (Figure 5A,B). Furthermore, miR-34a, miR-206-3p and miR-4510-5p were used to draw the Venn diagrams as their predicted target genes were ranked as the top three in ^{188}Re -liposome up-regulated microRNAs. Only one target, named *SLC44A2* encoded choline transporter-like protein 2 was co-regulated by these three microRNAs (Figure 5C). The same logic was used for ^{188}Re -liposome down-regulated microRNAs, and an only one target, named *U2SURP* encoded U2 snRNP-associated SURP motif-containing protein, was co-regulated by miR-142-5p, miR-194-5p and miR-944-3p (Figure 5D). Therefore, these bioinformatics analyses suggest that microRNAs and associated target genes of HPC tumors oppositely regulated by ^{188}Re -liposome are distinct.

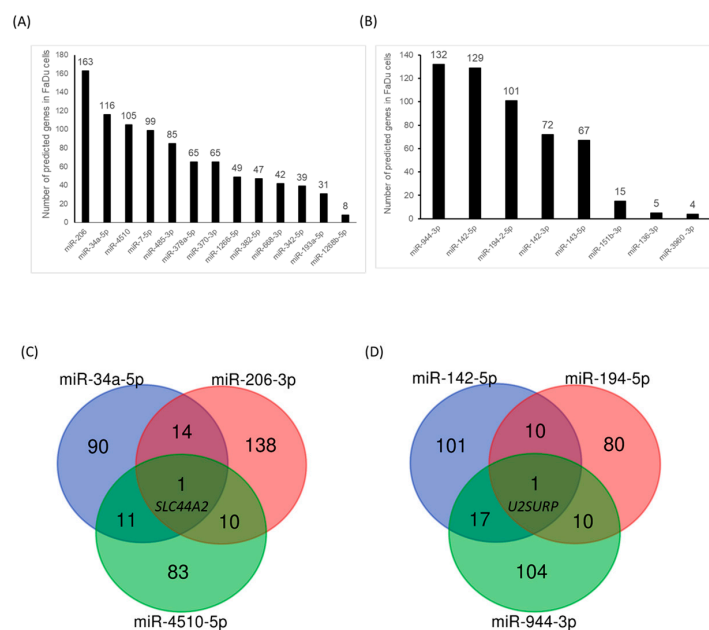


Figure 5. Analysis of miRNA-target interactions. (A) The individual target number of microRNAs up-regulated by ^{188}Re -liposome. (B) The individual target number of microRNAs down-regulated by ^{188}Re -liposome. (C,D) The Venn diagram calculated and drawn by the three microRNAs with the most targets.

2.6. Analysis of the Molecular Pathways Regulated by ^{188}Re -Liposome-Affected microRNA

We next used the pathview R package to investigate the genes influenced by microRNAs regulated by ^{188}Re -liposome. MicroRNA samples exhibiting over two-fold change were selected, and the affected target genes were subjected to the KEGG pathway database for determining the potent molecular pathways disturbed by ^{188}Re -liposome. We found that thirty pathways in resected HPC tumors were significantly affected by ^{188}Re -liposome ($p < 0.05$). The top three pathways with the lowest p values were genes involved in olfactory transduction, pathways in cancer, and taste transduction (Table 4). Additionally, ^{188}Re -liposome-influenced pathways could be categorized as cancer and carcinogenesis, cell adhesion and cytoskeletal organization, drug metabolism via cytochrome P450, tumor suppression and oncogenes. An integrated cancer pathway involved in the KEGG database was shown to demonstrate the related genes that could be regulated by ^{188}Re -liposome-induced or -suppressed microRNA expression (Figure 5). This revealed that genes associated with cell cycle progression, proliferation, and apoptosis were affected by ^{188}Re -liposome, including the down-regulation of *cyclin D*, *cyclin E*, cyclin-dependent kinase (CDK) 4/6, *E2F* transcription factor, and *bcl-2* anti-apoptotic factor, and the up-regulation of *p15*, *p16*, and *p27* cell cycle inhibitors and the *Rb* tumor suppressor gene (Figure 6). This pathway analysis provides a potent profile of the molecular mechanism for ^{188}Re -liposome regulated microRNA expression and tumor suppression of the HPC tumor model.

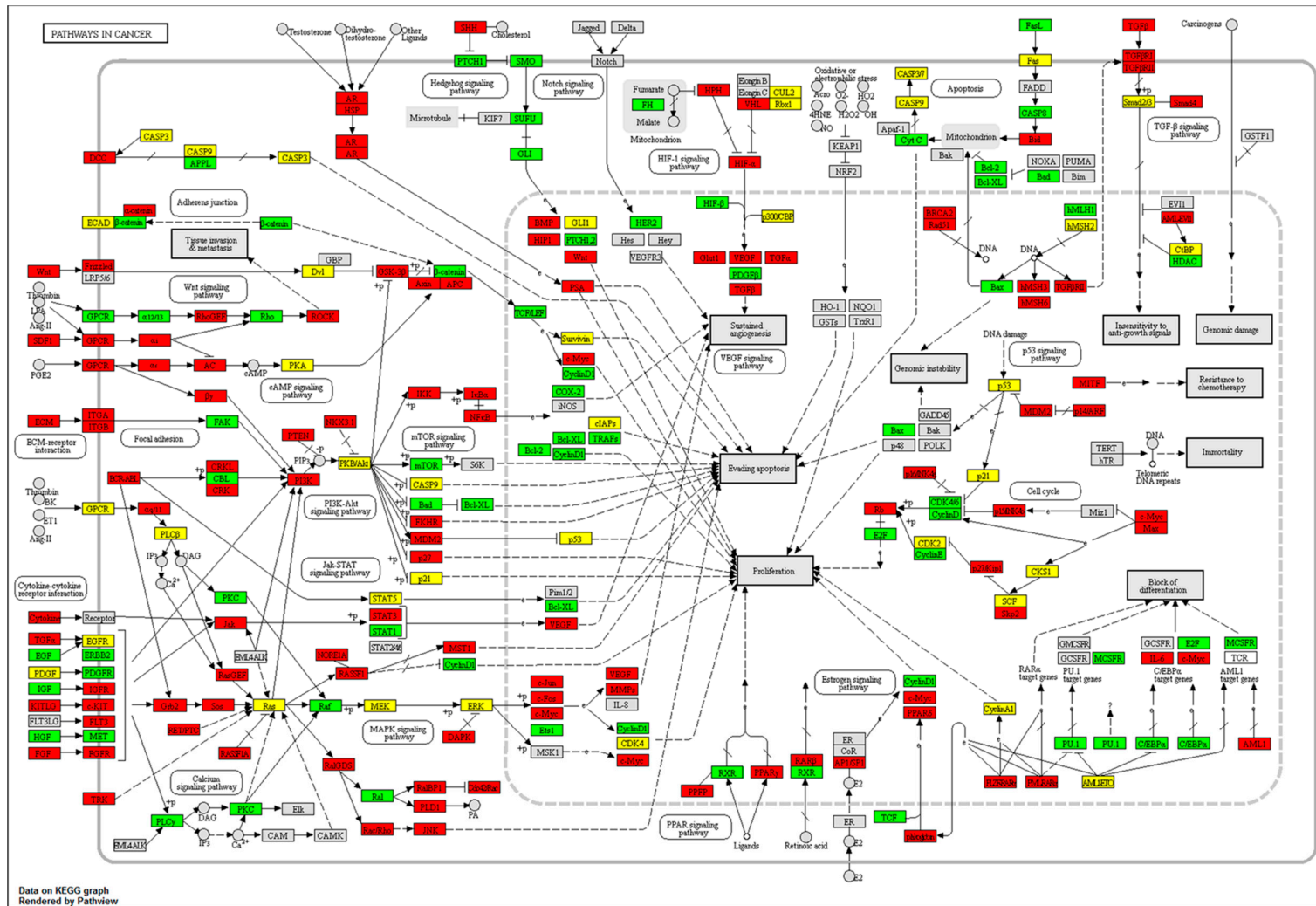


Figure 6. Use of the Kyoto Encyclopedia of Genes and Genomes (KEGG) database to display cancer pathway-associated genes affected by ¹⁸⁸Re-liposome mediated miRNA expression in HPC. Red: Up-regulated genes; green: down-regulated genes; yellow: unknown regulated genes; gray: unchanged genes.

Table 4. Thirty significant changed pathways after repeated doses of ¹⁸⁸Re-liposome treatment.

Pathways Description	No. of DEGs with Annotated Pathways (4498) ^a	Percentage of DEGs with Annotated Pathways (4498)	Down Regulated Gene	Up Regulated Gene	Unknown Regulated Gene	No. of All Genes with Annotated Pathways (6883)	Percentage of All Genes with Annotated Pathways (6883)	p-Value ^b
Olfactory transduction	51	1.13%	14	33	4	415	6.03%	6.37 × 10 ⁻⁴⁵
Pathways in cancer	329	7.31%	95	184	50	397	5.77%	0.00127
Taste transduction	16	0.36%	2	11	3	52	0.76%	0.00373
HTLV-I infection	217	4.82%	61	117	39	258	3.75%	0.00623
Proteoglycans in cancer	176	3.91%	60	93	23	203	2.95%	0.00739
Neuroactive ligand-receptor interaction	139	3.09%	40	84	15	277	4.02%	0.00779
MicroRNAs in cancer	151	3.36%	41	89	21	297	4.31%	0.00885
Viral carcinogenesis	175	3.89%	47	90	38	205	2.98%	0.0103
Chemical carcinogenesis	32	0.71%	4	21	7	81	1.18%	0.01124
Hippo signaling pathway	135	3.00%	34	82	19	154	2.24%	0.01459
Focal adhesion	174	3.87%	55	90	29	207	3.01%	0.01626
MAPK signaling pathway	209	4.65%	53	128	28	255	3.70%	0.01732
Drug metabolism - cytochrome P450	27	0.60%	5	17	5	68	0.99%	0.01947
Metabolism of xenobiotics by cytochrome P450	30	0.67%	4	20	6	74	1.08%	0.01954
ErbB signaling pathway	82	1.82%	30	40	12	87	1.26%	0.02121
Signaling pathways regulating pluripotency of stem cells	124	2.76%	29	80	15	142	2.06%	0.02202
Endocytosis	208	4.62%	65	116	27	258	3.75%	0.02587
FoxO signaling pathway	117	2.60%	32	75	10	134	1.95%	0.02612
Ras signaling pathway	185	4.11%	50	109	26	227	3.30%	0.0272
Neurotrophin signaling pathway	106	2.36%	28	64	14	120	1.74%	0.02764
Regulation of actin cytoskeleton	175	3.89%	49	98	28	214	3.11%	0.03031
Chronic myeloid leukemia	70	1.56%	22	40	8	73	1.06%	0.03053
Transcriptional misregulation in cancer	149	3.31%	43	80	26	179	2.60%	0.03365
Glioma	63	1.40%	23	30	10	65	0.94%	0.03554
Pancreatic cancer	64	1.42%	19	35	10	66	0.96%	0.03682
Colorectal cancer	60	1.33%	17	30	13	62	0.90%	0.03971
Acute myeloid leukemia	56	1.24%	17	28	11	57	0.83%	0.04123
Protein processing in endoplasmic reticulum	140	3.11%	40	78	22	169	2.46%	0.04447
Prostate cancer	80	1.78%	26	38	16	89	1.29%	0.04703
TGF-beta signaling pathway	76	1.69%	23	46	7	84	1.22%	0.04999

^a DEG: Differentially expressed genes. ^b Only $p < 0.05$ was counted.

2.7. Association of ^{188}Re -Liposome-Regulated microRNA and Patients' Survival Rate

As ^{188}Re -liposome could up-regulate tumor suppressive microRNA or down-regulate oncogenic microRNA of the HPC tumor model, we considered whether these microRNAs could be considered as prognostic factors for patients' survival rates. The microRNAs deregulated by ^{188}Re -liposome that displayed over five-fold change were examined. Notably, the online dataset only includes precursor forms of microRNAs for an analysis of patients' survival. For ^{188}Re -liposome up-regulated microRNAs in the HPC model, only miR-342 and miR-378a potentially exhibited an increase in the survival rate in HNSCC patients, with a marginal significance (Figure 7A,B). Interestingly, a high expression of miR-342 was significantly associated with a better survival rate in female patients (HR = 0.61, 95% CI = 0.38–0.98, $p = 0.038$). On the other hand, ^{188}Re -liposome down-regulated microRNAs, including miR-143, miR-6723, miR-944, and miR-136 were associated with a reduced survival rate in HNSCC patients when they were highly expressed (Figure 7C–F). Additionally, miR-3960 was also associated with reduced survival, yet the expression was too low for meaningful analysis (data not shown). These data suggest that specific miRNAs affected by ^{188}Re -liposome may be important for perspective clinical evaluation.

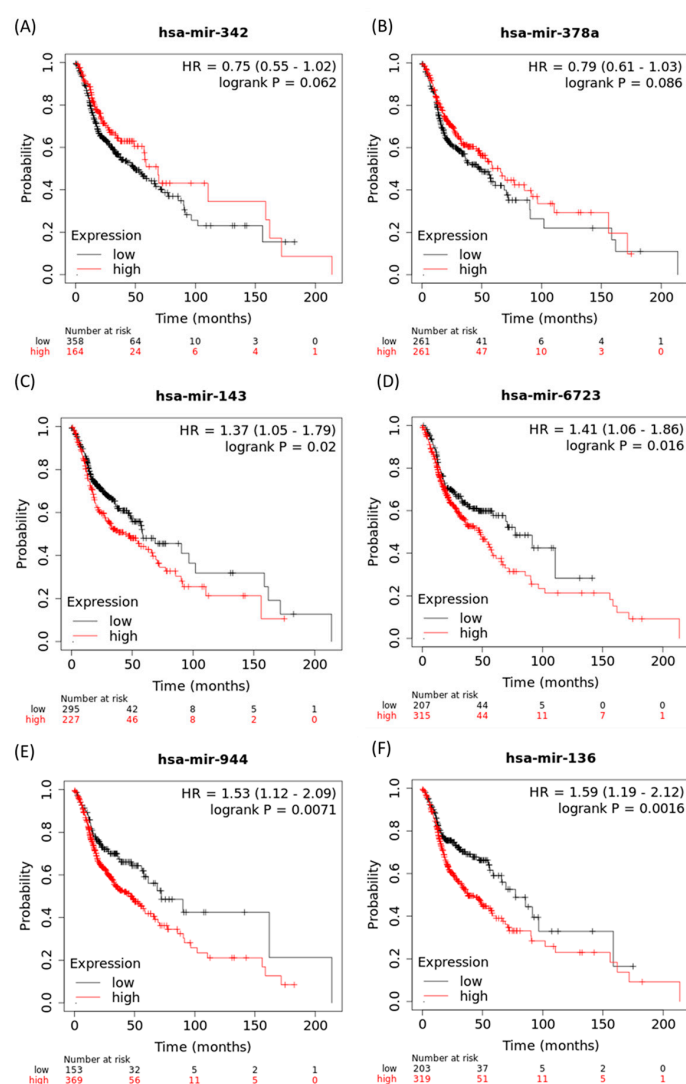


Figure 7. The association of ^{188}Re -liposome deregulated microRNAs with the survival rates of HNSCC patients. Kaplan–Meier (K-M) plot (A) hsa-miR-342; (B) hsa-miR-378a; (C) hsa-miR-143; (D) hsa-miR-6723; (E) hsa-miR-944; (F) hsa-miR-136.

3. Discussion

HPC mostly originates from mucosal squamous cells with a low incident rate. Because of unapparent early symptoms and a high metastatic ability, HPC accounts for the lowest survival rate of all head and neck cancers [72]. The FaDu cell line is a squamous cell carcinoma of the human hypopharynx commonly used for the study of molecular mechanisms of head and neck cancer in vitro and in vivo [73]. We have previously established an orthotopic tumor model using this cell line and found that *let-7* microRNA was associated with the therapeutic efficacy of ^{188}Re -liposome nanoparticles [24,74]. In this study, we used NGS analysis and found additional microRNAs that might be involved in the therapeutic efficacy of ^{188}Re -liposome after repeated administration. The expressions of the total RNA number and annotated small RNA were reduced in ^{188}Re -liposome treated tumors, suggesting that ^{188}Re -liposome would suppress gene transcription and expression.

As ^{188}Re is a high-energy β particles-emitter, it is expected to induce DNA damage. Indeed, the DNA damage marker γ H2AX was significantly induced by ^{188}Re -liposome compared to an untreated control. Interestingly, γ H2AX has been reported to be a tumor suppressor because of its role in the maintenance of genomic stability [75]. In our study, we found that ^{188}Re -liposome induced γ H2AX in HPC tumors. In the RNA-seq dataset, we also found that miR-138-2-5p, a potent inhibitor of H2AX [76], was down-regulated by over two-fold by ^{188}Re -liposome treatment. Together, these results are partially consistent with previous reports that might account for the therapeutic mechanisms of ^{188}Re -liposome from the viewpoint of γ -H2AX-mediated DNA damage responses.

According to the results of RNA-seq, ^{188}Re -liposome induced more than 200 microRNA to change their levels. To raise the selective criteria, we focused on the microRNA species exhibiting over five-fold up-regulation or down-regulation induced by ^{188}Re -liposome by comparing them to the untreated controls. The top three up-regulated microRNAs (miR-206-3p, miR-668-3p, and miR-485-3p) and down-regulated microRNAs (miR-142-5p, miR-944-3p, and miR-142-3p) displaying fold-change were categorized as tumor suppressors and oncogenes, respectively (Tables 2 and 3). Although miR-6723-5p was also highly suppressed by ^{188}Re -liposome, its role in cancer has not been interpreted in the dbDEMOC database or microRNA Cancer association database (miRCancer) [77]. Most of the microRNAs deregulated by ^{188}Re -liposome were expressed oppositely in HNSCC, and they were reported to be potent tumor suppressors or oncogenes in different types of cancers. However, there were no available data for miR-4510-5p, miR-1268b-5p, miR-6723-5p, miR-151b-3p, miR-143-5p, miR-194-2-5p and miR3960-3p in the database. As NGS is prominently used to find unknown genes that can be induced by treatment agents, the uncharacterized microRNAs shown to be significantly influenced by ^{188}Re -liposome treatment would be of interest for investigating their roles in the future.

The NGS analysis identified highly differentially expressed microRNAs that were also validated using FaDu tumors with or without ^{188}Re -liposome treatment, and clinical HNSCC samples using qPCR. The expression of analyzed microRNAs was consistent in these two different resources, although the case number of clinical samples was limited. The clinical information of the TCGA database could only be employed to analyze larynx cancer because the number of cases of HPC was too low to have normal tissues for analysis. Even so, we still found several microRNAs (e.g., miR-206-3p, miR-378-5p, and miR-142-5p) that were consistent with the results of NGS analysis and our clinical samples (Figure 4). In addition to ^{188}Re , ^{177}Lu is also a radionuclide that can emit 86% of β -particles and 14% of photons with a lower energy but longer half-life period. ^{177}Lu -octreotate has been reported to differentially regulate 57 specific microRNAs in mouse renal cortical tissue identified by the Mouse miRNA Oligo chip 4plex [78]. However, little microRNA was overlapped between their results and ours. Besides different types of radionuclides, the different animal models and microRNA mining methods may also account for the distinct observations in these two studies. Therefore, the differentially expressed microRNAs in the HPC model could be considered as specific prognostic factors for ^{188}Re -liposome treatment.

The predicted genes targeted by microRNAs were also analyzed by the miRDB public database. For the ^{188}Re -liposome up-regulated and down-regulated top three microRNAs, the *SLC44A2* gene

and *U2SURP* gene were the targets recognized by these oppositely regulated microRNAs, respectively. Hence, it is expected that *SLC44A2* would exhibit an oncogenic property and *U2SURP* should be a tumor suppressor gene. *SLC44A2*, first discovered in the inner ear, is a member of the choline transporter-like protein family of membrane transporter proteins [79,80]. *U2SURP* is involved in RNA splicing as it is part of spliceosomes [81]. However, little is known about the association of these two genes with human cancers. It would be an interesting target gene to investigate for its role in mediating the efficacy of ^{188}Re -liposome.

Using the KEGG pathway database, we found that 30 pathways in orthotopic HPC tumors were significantly influenced by ^{188}Re -liposome treatment. Although the cancer-suppression-related pathways were expected to be regulated by ^{188}Re -liposome, most of the affected genes in the annotated pathway displayed olfactory transduction. Radiation therapy has been reported to cause olfactory loss in head and neck cancer patients [82]. However, the conclusion is that radiation can damage olfactory cells. The position of hypopharyngeal cancer was not in the olfactory tract, yet FaDu cells were orthotopically injected into the buccal position of the mouse. This operation was based on the fact that FaDu cells are also buccal carcinoma cells [83]. Whether the microenvironmental difference influences the gene regulatory pathway of tumors is unclear. We believed that the excised tumor should not be contaminated by olfactory cells because the human tumor was very small after ^{188}Re -liposome treatment, that is, the tumor size was not big enough to reach the olfactory tract.

An assessment of the correlation between the gene expression and survival rate of patients is important for evaluating the clinical relevance of preclinical study for novel genes and drugs. Here we used the Kaplan–Meier plotter online tool that includes the datasets of TCGA program, the Gene Expression Omnibus (GEO) and the European Genome-Phenome Archive (EGA) to find the ^{188}Re -liposome regulated primary microRNAs and their association with patients' survival rates [84]. Although several potent tumor suppressive or oncogenic microRNAs were influenced by ^{188}Re -liposome, only part of these microRNAs exhibited the expected association with patients' survival probability in HNSCC. For instance, ^{188}Re -liposome suppressed miR-142 exhibited higher survival probabilities in HNSCC when they were expressed at higher levels, although they were expected to be oncogenic microRNAs [85]. A potent limitation is the sample size (523 cases) of HNSCC patients, which may be too small to draw conclusions on the role of microRNAs in patients' survival rates. Besides, the online K-M plotter only analyzes the effects of precursor microRNA on patients' survival rate. The association of mature miRNAs with the survival rate remains unknown. Whether different forms of the same microRNAs will differentially influence the results of the survival rate remains to be addressed.

In summary, current data suggest that the de-regulation of microRNAs correlates with the therapeutic efficacy of ^{188}Re -liposome on human HPC tumors. Using NGS, we also found several microRNAs that have not been fully characterized for their roles in cancer development and therapy. Whether these microRNAs are important for mediating the efficacy of ^{188}Re -liposome would be interesting to further investigate. Additionally, the KEGG pathway analysis showed that not only cancer pathways but also olfactory and taste transduction were significantly changed in HPC tumors after they were treated by ^{188}Re -liposome. Although no clinical evidence showing that patients treated with ^{188}Re -liposome will lose olfactory and gustatory sensation, olfactory sensory dysfunction and gustatory impairment often occur after patients are treated with radiotherapy in the head and neck area [82,86–89]. To the best of our knowledge, this is the first study uncovering the therapeutic mechanisms of ^{188}Re -liposome by an investigation of the pan-expression of microRNA. As ^{188}Re -liposome has entered the clinical trial stage, these data may further extend the concept of precise medicine using this radiotheranostic agent and allow the affected microRNAs to be prognostic factors after cancer treatment.

4. Materials and Methods

4.1. Cell Lines and Plasmid

Human FaDu HPC cells (American Type Culture Collection, Manassas, VA, USA) were cultured in RPMI-1640 (Life Technologies Inc., Carlsbad, CA, USA) containing 10% fetal bovine serum (FBS) (Thermo Fisher Scientific Inc., Waltham, MA, USA), 1% penicillin (Sigma-Aldrich Co., St. Louis, MO, USA), and 1% L-glutamine (Sigma-Aldrich Co., St. Louis, MO, USA). FaDu-3R cells harboring multiple reporter genes were used and cultured as reported previously [24]. Cells were incubated at 37°C in a humidified incubator with 5% CO₂ and passaged every two days.

4.2. Preparation of ¹⁸⁸Re-Liposome

The procedure of ¹⁸⁸Re-liposomal preparation has been reported before [23]. In brief, ¹⁸⁸Re was milked from the ¹⁸⁸W/¹⁸⁸Re generator system (Institute National des Radioelements, Fleurus, Belgium) and conjugated with sodium perrhenate. Moreover, ¹⁸⁸Re was conjugated with *N,N*-bis(2-mercapatoethyl)-*N',N'*-diethylenediamine (BMEDA, ABX GmbH, Radeberg, Germany), and the quality of ¹⁸⁸Re-BMEDA was validated by using the instant thin-layer chromatography (iTLC) followed by a radioactive scanner (Bioscan AR2000; Bioscan, TriFoil Imaging Inc., Chatsworth, CA, USA). Furthermore, PEGylated liposome (NanoX; Taiwan Liposome Co. Ltd., Taipei, Taiwan) was used to encapsulate ¹⁸⁸Re-BMEDA and eluted using the PD-10 column (GE Health BioSciences, Pittsburgh, PA, USA) (Supplementary Figure S1). The average molecular weight of polyethylene glycol (PEG) was 2000. The particle size (84.6 ± 4.12 nm) and surface charge (1.1 ± 1.9 mV) were measured by the dynamic light scattering apparatus (Zetasizer Nano ZS90, Malvern Panalytical Ltd., Malvern, UK). The *in vitro* stabilities of ¹⁸⁸Re-liposome in normal saline and rat plasma were, respectively, over 92% and 82% in 72 h as reported before [20].

4.3. Establishment of HPC Orthotopic Tumor Model for Evaluating the Therapeutic Efficacy of ¹⁸⁸Re-Liposome

Six-week-old male BALB/c nude mice (*N* = 5 for each experimental group) were purchased from National Laboratory Animal Center, Taipei, Taiwan and used for the establishment of orthotopic HPC tumor model. FaDu-3R cells (1 × 10⁶) were resuspended in 50 μL of OPTI-MEM (Sigma-Aldrich, St. Louis, MO, USA) and then injected into the buccal position of each mouse at right side using a 27 G insulin needle. For intravenous injection of ¹⁸⁸Re-liposome, 23.68 MBq (640 μCi) corresponding to 80% maximum tolerated dose (MTD), as we mentioned before [23]. To evaluate the therapeutic efficacy, the tumor viability and growth rate were measured using the luciferase reporter gene imaging and caliper measurement. The luminescent signals were acquired by the *In Vivo* Imaging System (*Optima*, Biospace Lab Inc., Paris, France). The tumor volume was calculated by the formula: (width² × length)/2 after caliper measurement every three days [90]. The animal experiments were approved by the Institutional Animal Care and Utilization Committee (IACUC) of National Yang-Ming University (No. 1061010).

4.4. Tumor Collection and Next-Generation Sequencing (NGS)

Tumors were harvested from tumor-bearing mice after four weeks of ¹⁸⁸Re-liposome treatment. Total RNA of both saline control and ¹⁸⁸Re-liposome treated group were extracted using the QIAGEN RNA mini kit (Thermo Fisher Scientific Inc., Waltham, MA, USA) according to manufacturer's instructions. Furthermore, the quality of RNA was detected using the Nanodrop spectrophotometer (Nanodrop Technologies LLC, Wilmington, DE, USA). The integrity and concentration of RNA samples were determined using the Agilent 2100 Bioanalyzer (Agilent Technologies, Santa Clara, CA, USA) with RNA 6000 nano kit (Agilent Technologies, Santa Clara, CA, USA). The TruSeq Small RNA Library kit (Illumina, Inc., San Diego, CA, USA) was then used to ligate RNA with adapters followed by the reverse transcription-PCR to generate cDNA library. The library was then sequenced by the HiSeq

4000 Sequencing System (2×150 bp paired-end Sequencing) and the results were processed with the Illumina software (Illumina, Inc., San Diego, CA, USA). To qualify the results of small RNA sequencing, the sequences were applied to the CLC Genomics Workbench v10 to obtain the qualified reads [91]. CLC Genomics Workbench counts different types of small RNAs in the data and compares them to databases of microRNAs or other small RNAs [92].

4.5. MicroRNA Expression Analysis

The 'miRBase' online source was used for the annotation of small RNA [93]. In the next step, all of the miRNAs were normalized by TMM (trimmed mean of M values) method using edgeR (R package: v.3.10.5) (Bioconductor, New York City, NY, USA) [94]. For a two-group experiment, we used the 'Fold Change' to tell how many times bigger the mean expression value in ^{188}Re -liposome group is relative to that of saline-only group. If the mean expression value in ^{188}Re -liposome group is small than that in saline-only group, the value will present negative sign, and vice versa. The criteria for microRNAs selection were fold change >5 .

4.6. Western Blot Analysis

Tumors were collected from the tumor-bearing mice after 4 weeks of ^{188}Re -liposome treatment, and lysed in T-PERTM Tissue Protein Extraction Reagent (Thermo Fisher Scientific, Waltham, MA, USA) containing 1% protease inhibitor cocktail (Sigma-Aldrich Co., St. Louis, MO, USA). Protein lysates (50 μg) were run on 8–12% SDS-PAGE, electro-transferred to nitrocellulose membrane, blocking and incubated with antibody as reported previously [95]. The primary antibodies were anti- γH2AX (GTX628789, GeneTex Inc., Irvine, CA, USA), and anti-glyceraldehyde3-phosphate dehydrogenase (GAPDH) (MA5-15738, Invitrogen Inc., Carlsbad, CA, USA).

4.7. Validation of microRNA Expression Using qPCR

To validate miRNA levels before and after HPC tumor treated with ^{188}Re -liposome and to compare normal tissue to HNSCC tissues using clinical samples, quantitative PCR (qPCR) of targeted miRNA was performed. Briefly, complementary DNA (cDNA) was generated from 2 μg total RNA using SuperScript II reverse transcriptase (Life-Technologies Co., Carlsbad, CA, USA). Then, the cDNA products were mixed with the Fast SYBR Green Master Mix (Life-Technologies Co., Carlsbad, CA, USA) and subjected to the StepOnePlus Real-time PCR System (Life-Technologies Co., Carlsbad, CA, USA) following the manufacturer's instructions. The sequences of stem loop primers, forward primers and universal primer used for miR-206-3p, miR-382-5p, miR-378a-5p, miR-3960-3p, and miR-142-5p amplification were summarized in Table 5. Use of human tissue samples was approved by the Institutional Review Board (No. 2019-01-010BC).

4.8. Heatmap Analysis of NGS Data

To gain the heatmap of total microRNAs' expression, 'TreeView' (v1.1.6r4) was used [96]. The heatmap analysis was based on the small RNA that has twice difference between individuals with or without the treatment of ^{188}Re -liposome, and then took Log₂ value to draw out.

4.9. Analysis of microRNA Using the Cancer Genome Atlas (TCGA)

The expression levels of miRNAs and clinical information for TCGA Head-Neck Squamous Cell Carcinoma (HNSC) were downloaded from Broad GDAC Firehose [97]. The miRNA expression values for samples having anatomic subdivision labeled as normal larynx tissue (12 cases), larynx cancers (117 cases) or hypopharynx cancers (10 cases) were used. In house R scripts were used to parse and generate heatmap and boxplots [98]. The difference between normal and tumor samples were tested with Wilcoxon signed-rank test.

Table 5. The list of stem loop primers, forward primers, and reverse primer used for qPCR of microRNAs.

MicroRNA	Stem Loop Primer Sequence
miR-206-3p	5'-GTCGTATCCAGTGCAGGGTCCGAG GTATTCGCACTGGATACGACCCACAC-3'
miR-382-5p	5'-GTCGTATCCAGTGCAGGGTCCGA GGTATTCGCACTGGATACGACCGAATC-3'
miR-378a-5p	5'-GTCGTATCCAGTGCAGGGTCCGAG GTATTCGCACTGGATACGACACACAG-3'
miR-3960-3p	5'-GTCGTATCCAGTGCAGGGTCCGAG GTATTCGCACTGGATACGACCCCCCG-3'
miR-142-5p	5'-GTCGTATCCAGTGCAGGGTCCGAG GTATTCGCACTGGATACGACAGTAGT-3'
MicroRNA	Forward Primer Sequence
miR-206-3p	5'-CACGCATGGAATGTAAGGAAGT-3'
miR-382-5p	5'-CACGCAGAAGTTGTTCTGTTGGT-3'
miR-378a-5p	5'-TGATTACTCCTGACTCCAGGTC-3'
miR-3960-3p	5'-TAATTATGGCGGCGGCGGAG-3'
miR-142-5p	5'-CACGCGCATAAAGTAGAAAGCA-3'
MicroRNA	Reverse Primer Sequence
Universal reverse primer	5'-CCAGTGCAGGGTCCGAGGT-3'

4.10. Characterization of miRNAs

The miRNA of interests were subjected to a Database of Differentially Expressed MiRNAs in human Cancer 2.0 (dbDEMC v2.0) that collects the data sets of Gene Expression Omnibus (GEO) and The Cancer Genome Atlas (TCGA) to exhibit differentially expressed miRNAs in human cancers detected by high throughput method [99]. The roles of miRNAs belonging to tumor suppressor genes or oncogenes were predicted accordingly. The miRDB online database for prediction of miRNA targets by a MirTarget bioinformatics tool was used to analyze putative downstream genes influenced by the miRNAs of interests [100,101]. Each microRNA was selected for target expression analysis for FaDu cells, and the targets expression level over 20 was counted as they were most relevant to FaDu cells. Target expression level was determined by RNA-Seq using the RPKM method (Reads Per Kilobase of transcript, per Million mapped reads). An online Venn diagrams drawing tool was exploited to calculate the intersections of list of miRNA targets [102].

4.11. The Pathway Analysis

The 'pathview' (R package: v1.4.2) software (Bioconductor, New York City, NY, USA) was used to draw pathways and find significant gene change (Fold change > 2) with the Kyoto Encyclopedia of Genes and Genomes (KEGG) [103,104]. Moreover, the pathways would be regarded significant if the *p*-value < 0.05.

4.12. Statistical Analysis

Statistical analysis was performed using GraphPad Prism 6.0 (GraphPad Software, San Diego, CA, USA). All data were represented as the means ± standard deviation (SD) with independent experiments. The Student's *t*-test was used for statistical analysis. Two-way Analysis of Variance (ANOVA) was used to compare the tumor growth curves. The Kaplan–Meier method with the log-rank test was used to analyze the association of miRNAs and patients' survival rates using the online K-M plotter with public datasets [84].

Supplementary Materials: The following are available online, Figure S1: Measurement of the combined efficiency between ^{188}Re and BMEDA chelator for embedding into liposome. Figure S2: Demonstration of reporter genes expression in FaDu-3R cells. Figure S3: Qualification of total RNA for NGS analysis. Figure S4: GC content analysis and sequencing qualification of RNA-Seq. Figure S5: A heatmap of differentially expressed microRNAs with or without ^{188}Re -liposomal treatment. Figure S6: A heatmap of selected differentially expressed microRNAs in normal tissues and larynx cancer tissues using the clinical information of TCGA.

Author Contributions: Conceptualization, Y.-J.L. and S.-Y.W.; methodology, B.-Z.L.; software, T.-W.C.; validation, B.-Z.L., M.-Y.L. and Y.-J.L.; formal analysis, B.-Z.L.; investigation, B.-Z.L.; resources, C.-H.C. and M.-H.Y.; data curation, M.-Y.L.; writing—original draft preparation, Y.-J.L.; writing—review and editing, Y.-J.L.; supervision, Y.-J.L. and S.-Y.W.; funding acquisition, Y.-J.L. and S.-Y.W. All authors have read and agreed to the published version of the manuscript.

Funding: This research was funded by National Yang-Ming University-Far Eastern Memorial Hospital Joint Research Program, grant number 108DN04; Ministry of Science and Technology grant number 105-2623-E-010-001-NU, 106-2623-E-010-002-NU, and 108-2314-B-010-016) and “The APC was funded by National Yang-Ming University-Far Eastern Memorial Hospital Joint Research Program”.

Acknowledgments: We thanked Shen-Nan Lo, Ming-Hsuan Lin for helping the ^{188}Re preparation, production, and quality assurance. We thank Liang-Ting Lin for discussion of references. We also thank the Taiwan Animal Consortium (MOST 106-2319-B-001-004)—Taiwan Mouse Clinic which is funded by the Ministry of Science and Technology (MOST) of Taiwan for technical support in in vivo imaging experiments. We also thank the support from the Cancer Progression Research Center, National Yang-Ming University, from the Featured Areas Research Center Program within the framework of the Higher Education Sprout Project by the Ministry of Education (MOE) in Taiwan.

Conflicts of Interest: The authors declare no conflict of interest.

References

1. Patel, R.S.; Goldstein, D.P.; Brown, D.; Irish, J.; Gullane, P.J.; Gilbert, R.W. Circumferential pharyngeal reconstruction: History, critical analysis of techniques, and current therapeutic recommendations. *Head Neck* **2010**, *32*, 109–120. [[CrossRef](#)] [[PubMed](#)]
2. Chu, P.Y.; Chang, S.Y. Reconstruction of the hypopharynx after surgical treatment of squamous cell carcinoma. *J. Chin. Med. Assoc.* **2009**, *72*, 351–355. [[CrossRef](#)]
3. Iwamoto, H. Operative treatment of cancer of the hypopharynx. *Gan No Rinsho* **1968**, *14*, 660–662. [[PubMed](#)]
4. Kim, S.; Wu, H.G.; Heo, D.S.; Kim, K.H.; Sung, M.W.; Park, C.I. Advanced hypopharyngeal carcinoma treatment results according to treatment modalities. *Head Neck* **2001**, *23*, 713–717. [[CrossRef](#)] [[PubMed](#)]
5. Mura, F.; Bertino, G.; Occhini, A.; Benazzo, M. Surgical treatment of hypopharyngeal cancer: A review of the literature and proposal for a decisional flow-chart. *Acta Otorhinolaryngol. Ital.* **2013**, *33*, 299–306. [[PubMed](#)]
6. Medvedeva, A.; Chernov, V.; Zeltchan, R.; Sinilkin, I.; Bragina, O.; Chijevskaya, S.; Choynzonov, E.; Goldberg, A. Nuclear medicine imaging of locally advanced laryngeal and hypopharyngeal cancer. In *AIP Conference Proceedings*; AIP Publishing LLC: Melville, NY, USA, 2017; Volume 1882.
7. Jadvar, H.; Chen, X.; Cai, W.; Mahmood, U. Radiotheranostics in Cancer Diagnosis and Management. *Radiology* **2018**, *286*, 388–400. [[CrossRef](#)]
8. Argyrou, M.; Valassi, A.; Andreou, M.; Lyra, M. Rhenium-188 production in hospitals, by w-188/re-188 generator, for easy use in radionuclide therapy. *Int. J. Mol. Imaging* **2013**, *2013*, 290750. [[CrossRef](#)]
9. Liepe, K.; Hliscs, R.; Kropp, J.; Gruning, T.; Runge, R.; Koch, R.; Knapp, F.F., Jr.; Franke, W.G. Rhenium-188-HEDP in the palliative treatment of bone metastases. *Cancer Biother. Radiopharm.* **2000**, *15*, 261–265. [[CrossRef](#)]
10. Zhang, H.; Tian, M.; Li, S.; Liu, J.; Tanada, S.; Endo, K. Rhenium-188-HEDP therapy for the palliation of pain due to osseous metastases in lung cancer patients. *Cancer Biother. Radiopharm.* **2003**, *18*, 719–726. [[CrossRef](#)]
11. Guerra Liberal, F.D.C.; Tavares, A.A.S.; Tavares, J. Palliative treatment of metastatic bone pain with radiopharmaceuticals: A perspective beyond Strontium-89 and Samarium-153. *Appl. Radiat. Isot.* **2016**, *110*, 87–99. [[CrossRef](#)]
12. Maxon, H.R., III; Schroder, L.E.; Washburn, L.C.; Thomas, S.R.; Samaritunga, R.C.; Biniakiewicz, D.; Moulton, J.S.; Cummings, D.; Ehrhardt, G.J.; Morris, V. Rhenium-188(Sn)HEDP for treatment of osseous metastases. *J. Nucl. Med.* **1998**, *39*, 659–663. [[PubMed](#)]
13. Uccelli, L.; Martini, P.; Pasquali, M.; Boschi, A. Monoclonal Antibodies Radiolabeling with Rhenium-188 for Radioimmunotherapy. *BioMed Res. Int.* **2017**, *2017*, 5923609. [[CrossRef](#)] [[PubMed](#)]

14. Edelman, M.J.; Clamon, G.; Kahn, D.; Magram, M.; Lister-James, J.; Line, B.R. Targeted radiopharmaceutical therapy for advanced lung cancer: Phase I trial of rhenium Re188 P2045, a somatostatin analog. *J. Thorac. Oncol.* **2009**, *4*, 1550–1554. [[CrossRef](#)] [[PubMed](#)]
15. Kumar, A.; Bal, C.; Srivastava, D.N.; Thulkar, S.P.; Sharma, S.; Acharya, S.K.; Duttagupta, S. Management of multiple intrahepatic recurrences after radiofrequency ablation of hepatocellular carcinoma with rhenium-188-HDD-lipiodol. *Eur. J. Gastroenterol. Hepatol.* **2006**, *18*, 219–223. [[CrossRef](#)] [[PubMed](#)]
16. Lambert, B.; Bacher, K.; De Keukeleire, K.; Smeets, P.; Colle, I.; Jeong, J.M.; Thierens, H.; Troisi, R.; De Vos, F.; Van de Wiele, C. 188Re-HDD/lipiodol for treatment of hepatocellular carcinoma: A feasibility study in patients with advanced cirrhosis. *J. Nucl. Med.* **2005**, *46*, 1326–1332. [[PubMed](#)]
17. Nowicki, M.L.; Cwikla, J.B.; Sankowski, A.J.; Shcherbinin, S.; Grimmes, J.; Celler, A.; Buscombe, J.R.; Bator, A.; Pech, M.; Mikolajczak, R.; et al. Initial study of radiological and clinical efficacy radioembolization using 188Re-human serum albumin (HSA) microspheres in patients with progressive, unresectable primary or secondary liver cancers. *Med. Sci. Monit.* **2014**, *20*, 1353–1362. [[CrossRef](#)]
18. Jeong, J.M.; Lee, Y.J.; Kim, E.H.; Chang, Y.S.; Kim, Y.J.; Son, M.; Lee, D.S.; Chung, J.K.; Lee, M.C. Preparation of (188) Re-labeled paper for treating skin cancer. *Appl. Radiat. Isot.* **2003**, *58*, 551–555. [[CrossRef](#)]
19. Wang, S.J.; Huang, W.S.; Chuang, C.M.; Chang, C.H.; Lee, T.W.; Ting, G.; Chen, M.H.; Chang, P.M.; Chao, T.C.; Teng, H.W.; et al. A phase 0 study of the pharmacokinetics, biodistribution, and dosimetry of (188)Re-liposome in patients with metastatic tumors. *Ejnmri. Res.* **2019**, *9*, 46. [[CrossRef](#)]
20. Chang, Y.J.; Chang, C.H.; Chang, T.J.; Yu, C.Y.; Chen, L.C.; Jan, M.L.; Luo, T.Y.; Lee, T.W.; Ting, G. Biodistribution, pharmacokinetics and microSPECT/CT imaging of 188Re-bMEDA-liposome in a C26 murine colon carcinoma solid tumor animal model. *Anticancer Res.* **2007**, *27*, 2217–2225.
21. Chang, C.H.; Liu, S.Y.; Chi, C.W.; Yu, H.L.; Chang, T.J.; Tsai, T.H.; Lee, T.W.; Chen, Y.J. External beam radiotherapy synergizes (1)(8)(8)Re-liposome against human esophageal cancer xenograft and modulates (1)(8)(8)Re-liposome pharmacokinetics. *Int. J. Nanomed.* **2015**, *10*, 3641–3649. [[CrossRef](#)]
22. Huang, F.Y.; Lee, T.W.; Chang, C.H.; Chen, L.C.; Hsu, W.H.; Chang, C.W.; Lo, J.M. Evaluation of 188Re-labeled PEGylated nanoliposome as a radionuclide therapeutic agent in an orthotopic glioma-bearing rat model. *Int. J. Nanomed.* **2015**, *10*, 463–473. [[CrossRef](#)]
23. Lin, L.T.; Chang, C.H.; Yu, H.L.; Liu, R.S.; Wang, H.E.; Chiu, S.J.; Chen, F.D.; Lee, T.W.; Lee, Y.J. Evaluation of the therapeutic and diagnostic effects of PEGylated liposome-embedded 188Re on human non-small cell lung cancer using an orthotopic small-animal model. *J. Nucl. Med.* **2014**, *55*, 1864–1870. [[CrossRef](#)]
24. Lin, L.T.; Chang, C.Y.; Chang, C.H.; Wang, H.E.; Chiou, S.H.; Liu, R.S.; Lee, T.W.; Lee, Y.J. Involvement of let-7 microRNA for the therapeutic effects of Rhenium-188-embedded liposomal nanoparticles on orthotopic human head and neck cancer model. *Oncotarget* **2016**, *7*, 65782–65796. [[CrossRef](#)]
25. Shen, Y.A.; Lan, K.L.; Chang, C.H.; Lin, L.T.; He, C.L.; Chen, P.H.; Lee, T.W.; Lee, Y.J.; Chuang, C.M. Intraperitoneal (188)Re-Liposome delivery switches ovarian cancer metabolism from glycolysis to oxidative phosphorylation and effectively controls ovarian tumour growth in mice. *Radiother. Oncol.* **2016**, *119*, 282–290. [[CrossRef](#)]
26. Chang, C.M.; Lan, K.L.; Huang, W.S.; Lee, Y.J.; Lee, T.W.; Chang, C.H.; Chuang, C.M. 188Re-Liposome Can Induce Mitochondrial Autophagy and Reverse Drug Resistance for Ovarian Cancer: From Bench Evidence to Preliminary Clinical Proof-of-Concept. *Int. J. Mol. Sci.* **2017**, *18*, 903. [[CrossRef](#)]
27. Rutman, A.M.; Kuo, M.D. Radiogenomics: Creating a link between molecular diagnostics and diagnostic imaging. *Eur. J. Radiol.* **2009**, *70*, 232–241. [[CrossRef](#)]
28. Kang, J.; Rancati, T.; Lee, S.; Oh, J.H.; Kerns, S.L.; Scott, J.G.; Schwartz, R.; Kim, S.; Rosenstein, B.S. Machine Learning and Radiogenomics: Lessons Learned and Future Directions. *Front. Oncol.* **2018**, *8*, 228. [[CrossRef](#)]
29. Lawrence, M.S.; Stojanov, P.; Mermel, C.H.; Robinson, J.T.; Garraway, L.A.; Golub, T.R.; Meyerson, M.; Gabriel, S.B.; Lander, E.S.; Getz, G. Discovery and saturation analysis of cancer genes across 21 tumour types. *Nature* **2014**, *505*, 495–501. [[CrossRef](#)]
30. Schulze, K.; Nault, J.C.; Villanueva, A. Genetic profiling of hepatocellular carcinoma using next-generation sequencing. *J. Hepatol.* **2016**, *65*, 1031–1042. [[CrossRef](#)]
31. Wang, Z.; Gerstein, M.; Snyder, M. RNA-Seq: A revolutionary tool for transcriptomics. *Nat. Rev. Genet.* **2009**, *10*, 57–63. [[CrossRef](#)]
32. Roh, S.W.; Abell, G.C.; Kim, K.H.; Nam, Y.D.; Bae, J.W. Comparing microarrays and next-generation sequencing technologies for microbial ecology research. *Trends Biotechnol.* **2010**, *28*, 291–299. [[CrossRef](#)]

33. Doostparast Torshizi, A.; Wang, K. Next-generation sequencing in drug development: Target identification and genetically stratified clinical trials. *Drug Discov. Today* **2018**, *23*, 1776–1783. [[CrossRef](#)]
34. Liu, F.; Zhao, X.; Qian, Y.; Zhang, J.; Zhang, Y.; Yin, R. MiR-206 inhibits Head and neck squamous cell carcinoma cell progression by targeting HDAC6 via PTEN/AKT/mTOR pathway. *Biomed. Pharm.* **2017**, *96*, 229–237. [[CrossRef](#)]
35. Koshizuka, K.; Hanazawa, T.; Fukumoto, I.; Kikkawa, N.; Matsushita, R.; Mataka, H.; Mizuno, K.; Okamoto, Y.; Seki, N. Dual-receptor (EGFR and c-MET) inhibition by tumor-suppressive miR-1 and miR-206 in head and neck squamous cell carcinoma. *J. Hum. Genet.* **2017**, *62*, 113–121. [[CrossRef](#)]
36. Momen-Heravi, F.; Trachtenberg, A.J.; Kuo, W.P.; Cheng, Y.S. Genomewide Study of Salivary MicroRNAs for Detection of Oral Cancer. *J. Dent. Res.* **2014**, *93*, 86S–93S. [[CrossRef](#)]
37. Shin, K.H.; Pucar, A.; Kim, R.H.; Bae, S.D.; Chen, W.; Kang, M.K.; Park, N.H. Identification of senescence-inducing microRNAs in normal human keratinocytes. *Int. J. Oncol.* **2011**, *39*, 1205–1211. [[CrossRef](#)]
38. Lou, C.; Xiao, M.; Cheng, S.; Lu, X.; Jia, S.; Ren, Y.; Li, Z. MiR-485-3p and miR-485-5p suppress breast cancer cell metastasis by inhibiting PGC-1 α expression. *Cell Death Dis.* **2016**, *7*, e2159. [[CrossRef](#)]
39. Wang, Z.Q.; Zhang, M.Y.; Deng, M.L.; Weng, N.Q.; Wang, H.Y.; Wu, S.X. Low serum level of miR-485-3p predicts poor survival in patients with glioblastoma. *PLoS ONE* **2017**, *12*, e0184969. [[CrossRef](#)]
40. Zhang, Y.; Sui, R.; Chen, Y.; Liang, H.; Shi, J.; Piao, H. Downregulation of miR-485-3p promotes glioblastoma cell proliferation and migration via targeting RNF135. *Exp. Med.* **2019**, *18*, 475–482. [[CrossRef](#)]
41. Wang, J.; Chen, C.; Yan, X.; Wang, P. The role of miR-382-5p in glioma cell proliferation, migration and invasion. *Onco. Targets* **2019**, *12*, 4993–5002. [[CrossRef](#)]
42. Feng, J.; Qi, B.; Guo, L.; Chen, L.Y.; Wei, X.F.; Liu, Y.Z.; Zhao, B.S. miR-382 functions as a tumor suppressor against esophageal squamous cell carcinoma. *World J. Gastroenterol.* **2017**, *23*, 4243–4251. [[CrossRef](#)]
43. Zhu, W.J.; Chen, X.; Wang, Y.W.; Liu, H.T.; Ma, R.R.; Gao, P. MiR-1268b confers chemosensitivity in breast cancer by targeting ERBB2-mediated PI3K-AKT pathway. *Oncotarget* **2017**, *8*, 89631–89642. [[CrossRef](#)]
44. Pu, Y.; Zhao, F.; Cai, W.; Meng, X.; Li, Y.; Cai, S. MiR-193a-3p and miR-193a-5p suppress the metastasis of human osteosarcoma cells by down-regulating Rab27B and SRR, respectively. *Clin. Exp. Metastasis* **2016**, *33*, 359–372. [[CrossRef](#)]
45. Chou, N.H.; Lo, Y.H.; Wang, K.C.; Kang, C.H.; Tsai, C.Y.; Tsai, K.W. MiR-193a-5p and -3p Play a Distinct Role in Gastric Cancer: miR-193a-3p Suppresses Gastric Cancer Cell Growth by Targeting ETS1 and CCND1. *Anticancer Res.* **2018**, *38*, 3309–3318. [[CrossRef](#)]
46. Yin, C.Y.; Kong, W.; Jiang, J.; Xu, H.; Zhao, W. miR-7-5p inhibits cell migration and invasion in glioblastoma through targeting SATB1. *Oncol. Lett.* **2019**, *17*, 1819–1825. [[CrossRef](#)]
47. Shi, Y.; Luo, X.; Li, P.; Tan, J.; Wang, X.; Xiang, T.; Ren, G. miR-7-5p suppresses cell proliferation and induces apoptosis of breast cancer cells mainly by targeting REGgamma. *Cancer Lett.* **2015**, *358*, 27–36. [[CrossRef](#)]
48. Wang, Z.; Ma, B.; Ji, X.; Deng, Y.; Zhang, T.; Zhang, X.; Gao, H.; Sun, H.; Wu, H.; Chen, X.; et al. MicroRNA-378-5p suppresses cell proliferation and induces apoptosis in colorectal cancer cells by targeting BRAF. *Cancer Cell Int.* **2015**, *15*, 40. [[CrossRef](#)]
49. Li, H.; Dai, S.; Zhen, T.; Shi, H.; Zhang, F.; Yang, Y.; Kang, L.; Liang, Y.; Han, A. Clinical and biological significance of miR-378a-3p and miR-378a-5p in colorectal cancer. *Eur. J. Cancer.* **2014**, *50*, 1207–1221. [[CrossRef](#)]
50. Ostadrahimi, S.; Abedi Valugerdi, M.; Hassan, M.; Haddad, G.; Fayaz, S.; Parvizhamidi, M.; Mahdian, R.; Fard Esfahani, P. miR-1266-5p and miR-185-5p Promote Cell Apoptosis in Human Prostate Cancer Cell Lines. *Asian Pac. J. Cancer Prev.* **2018**, *19*, 2305–2311. [[CrossRef](#)]
51. Shen, X.P.; Ling, X.; Lu, H.; Zhou, C.X.; Zhang, J.K.; Yu, Q. Low expression of microRNA-1266 promotes colorectal cancer progression via targeting FTO. *Eur. Rev. Med. Pharm. Sci.* **2018**, *22*, 8220–8226. [[CrossRef](#)]
52. Hironaka-Mitsuhashi, A.; Matsuzaki, J.; Takahashi, R.U.; Yoshida, M.; Nezu, Y.; Yamamoto, Y.; Shiino, S.; Kinoshita, T.; Ushijima, T.; Hiraoka, N.; et al. A tissue microRNA signature that predicts the prognosis of breast cancer in young women. *PLoS ONE* **2017**, *12*, e0187638. [[CrossRef](#)] [[PubMed](#)]
53. Chen, L.; Yuan, L.; Wang, G.; Cao, R.; Peng, J.; Shu, B.; Qian, G.; Wang, X.; Xiao, Y. Identification and bioinformatics analysis of miRNAs associated with human muscle invasive bladder cancer. *Mol. Med. Rep.* **2017**, *16*, 8709–8720. [[CrossRef](#)] [[PubMed](#)]

54. Pedersen, N.J.; Jensen, D.H.; Lelkaitis, G.; Kiss, K.; Charabi, B.W.; Ullum, H.; Specht, L.; Schmidt, A.Y.; Nielsen, F.C.; von Buchwald, C. MicroRNA-based classifiers for diagnosis of oral cavity squamous cell carcinoma in tissue and plasma. *Oral. Oncol.* **2018**, *83*, 46–52. [[CrossRef](#)] [[PubMed](#)]
55. Wang, X.; Zhao, Y.; Lu, Q.; Fei, X.; Lu, C.; Li, C.; Chen, H. MiR-34a-5p Inhibits Proliferation, Migration, Invasion and Epithelial-mesenchymal Transition in Esophageal Squamous Cell Carcinoma by Targeting LEF1 and Inactivation of the Hippo-YAP1/TAZ Signaling Pathway. *J. Cancer* **2020**, *11*, 3072–3081. [[CrossRef](#)] [[PubMed](#)]
56. Gao, J.; Li, N.; Dong, Y.; Li, S.; Xu, L.; Li, X.; Li, Y.; Li, Z.; Ng, S.S.; Sung, J.J.; et al. miR-34a-5p suppresses colorectal cancer metastasis and predicts recurrence in patients with stage II/III colorectal cancer. *Oncogene* **2015**, *34*, 4142–4152. [[CrossRef](#)] [[PubMed](#)]
57. Yang, H.; Li, Q.; Niu, J.; Li, B.; Jiang, D.; Wan, Z.; Yang, Q.; Jiang, F.; Wei, P.; Bai, S. microRNA-342-5p and miR-608 inhibit colon cancer tumorigenesis by targeting NAA10. *Oncotarget* **2016**, *7*, 2709–2720. [[CrossRef](#)]
58. Soriano, A.; Masanas, M.; Boloix, A.; Masia, N.; Paris-Coderch, L.; Piskareva, O.; Jimenez, C.; Henrich, K.O.; Roma, J.; Westermann, F.; et al. Functional high-throughput screening reveals miR-323a-5p and miR-342-5p as new tumor-suppressive microRNA for neuroblastoma. *Cell Mol. Life Sci.* **2019**, *76*, 2231–2243. [[CrossRef](#)]
59. He, Z.; Yi, J.; Liu, X.; Chen, J.; Han, S.; Jin, L.; Chen, L.; Song, H. MiR-143-3p functions as a tumor suppressor by regulating cell proliferation, invasion and epithelial-mesenchymal transition by targeting QKI-5 in esophageal squamous cell carcinoma. *Mol. Cancer* **2016**, *15*, 51. [[CrossRef](#)]
60. Jin, X.; Chen, X.; Hu, Y.; Ying, F.; Zou, R.; Lin, F.; Shi, Z.; Zhu, X.; Yan, X.; Li, S.; et al. LncRNA-TCONS_00026907 is involved in the progression and prognosis of cervical cancer through inhibiting miR-143-5p. *Cancer Med.* **2017**, *6*, 1409–1423. [[CrossRef](#)]
61. Yang, F.; Xiao, Z.; Zhang, S. Knockdown of miR-194-5p inhibits cell proliferation, migration and invasion in breast cancer by regulating the Wnt/beta-catenin signaling pathway. *Int. J. Mol. Med.* **2018**, *42*, 3355–3363. [[CrossRef](#)]
62. Jiang, M.J.; Chen, Y.Y.; Dai, J.J.; Gu, D.N.; Mei, Z.; Liu, F.R.; Huang, Q.; Tian, L. Dying tumor cell-derived exosomal miR-194-5p potentiates survival and repopulation of tumor repopulating cells upon radiotherapy in pancreatic cancer. *Mol. Cancer* **2020**, *19*, 68. [[CrossRef](#)] [[PubMed](#)]
63. Kosela-Paterczyk, H.; Paziewska, A.; Kulecka, M.; Balabas, A.; Kluska, A.; Dabrowska, M.; Piatkowska, M.; Zeber-Lubecka, N.; Ambrozkiwicz, F.; Karczmariski, J.; et al. Signatures of circulating microRNA in four sarcoma subtypes. *J. Cancer* **2020**, *11*, 874–882. [[CrossRef](#)] [[PubMed](#)]
64. Gullu Amuran, G.; Tinay, I.; Filinte, D.; Ilgin, C.; Peker Eyuboglu, I.; Akkiprik, M. Urinary micro-RNA expressions and protein concentrations may differentiate bladder cancer patients from healthy controls. *Int. Urol. Nephrol.* **2020**, *52*, 461–468. [[CrossRef](#)] [[PubMed](#)]
65. Chen, X.; Huang, Z.; Chen, R. MicroRNA-136 promotes proliferation and invasion in gastric cancer cells through Pten/Akt/P-Akt signaling pathway. *Oncol. Lett.* **2018**, *15*, 4683–4689. [[CrossRef](#)] [[PubMed](#)]
66. Li, Y.; Chen, D.; Jin, L.U.; Liu, J.; Li, Y.; Su, Z.; Qi, Z.; Shi, M.; Jiang, Z.; Yang, S.; et al. Oncogenic microRNA-142-3p is associated with cellular migration, proliferation and apoptosis in renal cell carcinoma. *Oncol. Lett.* **2016**, *11*, 1235–1241. [[CrossRef](#)] [[PubMed](#)]
67. Zhang, H.; Li, T.; Zheng, L.; Huang, X. Biomarker MicroRNAs for Diagnosis of Oral Squamous Cell Carcinoma Identified Based on Gene Expression Data and MicroRNA-mRNA Network Analysis. *Comput. Math Methods Med.* **2017**, *2017*, 9803018. [[CrossRef](#)]
68. Park, S.; Kim, J.; Eom, K.; Oh, S.; Kim, S.; Kim, G.; Ahn, S.; Park, K.H.; Chung, D.; Lee, H. microRNA-944 overexpression is a biomarker for poor prognosis of advanced cervical cancer. *Bmc Cancer* **2019**, *19*, 419. [[CrossRef](#)]
69. He, H.; Tian, W.; Chen, H.; Jiang, K. MiR-944 functions as a novel oncogene and regulates the chemoresistance in breast cancer. *Tumour Biol.* **2016**, *37*, 1599–1607. [[CrossRef](#)]
70. Ma, Z.; Liu, T.; Huang, W.; Liu, H.; Zhang, H.M.; Li, Q.; Chen, Z.; Guo, A.Y. MicroRNA regulatory pathway analysis identifies miR-142-5p as a negative regulator of TGF-beta pathway via targeting SMAD3. *Oncotarget* **2016**, *7*, 71504–71513. [[CrossRef](#)]
71. Islam, F.; Gopalan, V.; Vider, J.; Lu, C.T.; Lam, A.K. MiR-142-5p act as an oncogenic microRNA in colorectal cancer: Clinicopathological and functional insights. *Exp. Mol. Pathol.* **2018**, *104*, 98–107. [[CrossRef](#)]

72. Lamperska, K.M.; Kolenda, T.; Teresiak, A.; Kowalik, A.; Kruszyna-Mochalska, M.; Jackowiak, W.; Blizniak, R.; Przybyla, W.; Kapalczyńska, M.; Kozłowski, P. Different levels of let-7d expression modulate response of FaDu cells to irradiation and chemotherapeutics. *PLoS ONE* **2017**, *12*, e0180265. [[CrossRef](#)] [[PubMed](#)]
73. Rangan, S.R. A new human cell line (FaDu) from a hypopharyngeal carcinoma. *Cancer* **1972**, *29*, 117–121. [[CrossRef](#)]
74. Chang, C.Y.; Chen, C.C.; Lin, L.T.; Chang, C.H.; Chen, L.C.; Wang, H.E.; Lee, T.W.; Lee, Y.J. PEGylated liposome-encapsulated rhenium-188 radiopharmaceutical inhibits proliferation and epithelial-mesenchymal transition of human head and neck cancer cells in vivo with repeated therapy. *Cell Death Discov.* **2018**, *4*, 100. [[CrossRef](#)] [[PubMed](#)]
75. Bonner, W.M.; Redon, C.E.; Dickey, J.S.; Nakamura, A.J.; Sedelnikova, O.A.; Solier, S.; Pommier, Y. GammaH2AX and cancer. *Nat. Rev. Cancer* **2008**, *8*, 957–967. [[CrossRef](#)]
76. Wang, Y.; Huang, J.W.; Li, M.; Cavenee, W.K.; Mitchell, P.S.; Zhou, X.; Tewari, M.; Furnari, F.B.; Taniguchi, T. MicroRNA-138 modulates DNA damage response by repressing histone H2AX expression. *Mol. Cancer Res.* **2011**, *9*, 1100–1111. [[CrossRef](#)]
77. Xie, B.; Ding, Q.; Han, H.; Wu, D. miRCancer: A microRNA-cancer association database constructed by text mining on literature. *Bioinformatics* **2013**, *29*, 638–644. [[CrossRef](#)]
78. Schuler, E.; Parris, T.Z.; Helou, K.; Forssell-Aronsson, E. Distinct microRNA expression profiles in mouse renal cortical tissue after 177Lu-octreotate administration. *PLoS ONE* **2014**, *9*, e112645. [[CrossRef](#)]
79. Zajic, G.; Nair, T.S.; Ptok, M.; Van Waes, C.; Altschuler, R.A.; Schacht, J.; Carey, T.E. Monoclonal antibodies to inner ear antigens: I. Antigens expressed by supporting cells of the guinea pig cochlea. *Hear. Res.* **1991**, *52*, 59–71. [[CrossRef](#)]
80. He, L.; Vasilou, K.; Nebert, D.W. Analysis and update of the human solute carrier (SLC) gene superfamily. *Hum. Genom.* **2009**, *3*, 195–206. [[CrossRef](#)]
81. De Maio, A.; Yalamanchili, H.K.; Adamski, C.J.; Gennarino, V.A.; Liu, Z.; Qin, J.; Jung, S.Y.; Richman, R.; Orr, H.; Zoghbi, H.Y. RBM17 Interacts with U2SURP and CHERP to Regulate Expression and Splicing of RNA-Processing Proteins. *Cell Rep.* **2018**, *25*, 726–736.e7. [[CrossRef](#)]
82. Bramerson, A.; Nyman, J.; Nordin, S.; Bende, M. Olfactory loss after head and neck cancer radiation therapy. *Rhinology* **2013**, *51*, 206–209. [[CrossRef](#)] [[PubMed](#)]
83. Reiss, M.; Stash, E.B.; Vellucci, V.F.; Zhou, Z.L. Activation of the autocrine transforming growth factor alpha pathway in human squamous carcinoma cells. *Cancer Res.* **1991**, *51*, 6254–6262. [[PubMed](#)]
84. Nagy, A.; Lanczky, A.; Menyhart, O.; Gyorffy, B. Author Correction: Validation of miRNA prognostic power in hepatocellular carcinoma using expression data of independent datasets. *Sci. Rep.* **2018**, *8*, 11515. [[CrossRef](#)] [[PubMed](#)]
85. Chang, S.S.; Jiang, W.W.; Smith, I.; Poeta, L.M.; Begum, S.; Glazer, C.; Shan, S.; Westra, W.; Sidransky, D.; Califano, J.A. MicroRNA alterations in head and neck squamous cell carcinoma. *Int. J. Cancer* **2008**, *123*, 2791–2797. [[CrossRef](#)] [[PubMed](#)]
86. Sagar, S.M.; Thomas, R.J.; Loverock, L.T.; Spittle, M.F. Olfactory sensations produced by high-energy photon irradiation of the olfactory receptor mucosa in humans. *Int. J. Radiat. Oncol. Biol. Phys.* **1991**, *20*, 771–776. [[CrossRef](#)]
87. Hua, M.S.; Chen, S.T.; Tang, L.M.; Leung, W.M. Olfactory function in patients with nasopharyngeal carcinoma following radiotherapy. *Brain Inj.* **1999**, *13*, 905–915. [[CrossRef](#)] [[PubMed](#)]
88. Ruo Redda, M.G.; Allis, S. Radiotherapy-induced taste impairment. *Cancer Treat. Rev.* **2006**, *32*, 541–547. [[CrossRef](#)]
89. Epstein, J.B.; Smutzer, G.; Doty, R.L. Understanding the impact of taste changes in oncology care. *Support. Care Cancer* **2016**, *24*, 1917–1931. [[CrossRef](#)]
90. Carlsson, G.; Gullberg, B.; Hafström, L. Estimation of liver tumor volume using different formulas—An experimental study in rats. *J. Cancer Res. Clin. Oncol.* **1983**, *105*, 20–23. [[CrossRef](#)]
91. Andrews, S.; Krueger, F.; Segonds-Pichon, A.; Biggins, L.; Krueger, C.; Wingett, S.; Montgomery, J. Babraham Bioinformatics-Fastqc a Quality Control Tool For High Throughput Sequence Data. Available online: <http://www.bioinformatics.babraham.ac.uk/projects/fastqc/> (accessed on 22 January 2019).
92. Creighton, C.J.; Reid, J.G.; Gunaratne, P.H. Expression profiling of microRNAs by deep sequencing. *Brief. Bioinform.* **2009**, *10*, 490–497. [[CrossRef](#)]

93. Ambros, V.; Bartel, B.; Bartel, D.P.; Burge, C.B.; Carrington, J.C.; Chen, X.; Dreyfuss, G.; Eddy, S.R.; Griffiths-Jones, S.; Marshall, M.; et al. A uniform system for microRNA annotation. *RNA* **2003**, *9*, 277–279. [[CrossRef](#)] [[PubMed](#)]
94. Robinson, M.D.; McCarthy, D.J.; Smyth, G.K. edgeR: A Bioconductor package for differential expression analysis of digital gene expression data. *Bioinformatics* **2010**, *26*, 139–140. [[CrossRef](#)] [[PubMed](#)]
95. Tsai, C.H.; Lin, L.T.; Wang, C.Y.; Chiu, Y.W.; Chou, Y.T.; Chiu, S.J.; Wang, H.E.; Liu, R.S.; Wu, C.Y.; Chan, P.C.; et al. Over-expression of cofilin-1 suppressed growth and invasion of cancer cells is associated with up-regulation of let-7 microRNA. *Biochim. Biophys. Acta* **2015**, *1852*, 851–861. [[CrossRef](#)] [[PubMed](#)]
96. Saldanha, A.J. Java Treeview-extensible visualization of microarray data. *Bioinformatics* **2004**, *20*, 3246–3248. [[CrossRef](#)]
97. Deng, M.; Bragelmann, J.; Kryukov, I.; Saraiva-Agostinho, N.; Perner, S. FirebrowseR: An R client to the Broad Institute’s Firehose Pipeline. *Database* **2017**, *2017*, baw160. [[CrossRef](#)]
98. Wickham, H. *ggplot2: Elegant Graphics for Data Analysis*; Springer: New York, NY, USA, 2016.
99. Yang, Z.; Wu, L.; Wang, A.; Tang, W.; Zhao, Y.; Zhao, H.; Teschendorff, A.E. dbDEMC 2.0: Updated database of differentially expressed miRNAs in human cancers. *Nucleic Acids Res.* **2017**, *45*, D812–D818. [[CrossRef](#)]
100. Chen, Y.; Wang, X. miRDB: An online database for prediction of functional microRNA targets. *Nucleic Acids Res.* **2020**, *48*, D127–D131. [[CrossRef](#)]
101. Liu, W.; Wang, X. Prediction of functional microRNA targets by integrative modeling of microRNA binding and target expression data. *Genome Biol.* **2019**, *20*, 18. [[CrossRef](#)]
102. Lieven Sterck, V.d.P.Y. Draw Venn Diagram-Bioinformatics.psb.ugent.be. Available online: <http://bioinformatics.psb.ugent.be/webtools/Venn/> (accessed on 25 June 2020).
103. Kanehisa, M.; Sato, Y.; Kawashima, M.; Furumichi, M.; Tanabe, M. KEGG as a reference resource for gene and protein annotation. *Nucleic Acids Res.* **2016**, *44*, D457–D462. [[CrossRef](#)]
104. Kanehisa, M.; Sato, Y.; Morishima, K. BlastKOALA and GhostKOALA: KEGG Tools for Functional Characterization of Genome and Metagenome Sequences. *J. Mol. Biol.* **2016**, *428*, 726–731. [[CrossRef](#)]

Sample Availability: Samples of the compounds BMEDA and liposomes are available from the authors.



© 2020 by the authors. Licensee MDPI, Basel, Switzerland. This article is an open access article distributed under the terms and conditions of the Creative Commons Attribution (CC BY) license (<http://creativecommons.org/licenses/by/4.0/>).